"BABEŞ-BOLYAI" UNIVERSITY
CLUJ-NAPOCA

Faculty of Chemistry and Chemical Engineering
Chemistry Doctoral School

SYNTHESIS AND CHARACTERIZATION OF SOME POLYOXOMETALATES WITH POSSIBLE BIOLOGICAL APPLICATIONS

PhD Thesis Summary

Scientific supervisor:

Professor Mariana RUSU, MSc, PhD

PhD Student:

Silvia-Ştefana Bâlici

CLUJ-NAPOCA
2015

PhD Commission for Mrs. Silvia-Ştefana Ş. Bâlici

President:

Professor Anca Silvestru, MSc, PhD
Faculty of Chemistry and Chemical Engineering,
"Babeş-Bolyai" University, Cluj-Napoca

Scientific supervisor:

Professor Mariana RUSU, MSc, PhD
Faculty of Chemistry and Chemical Engineering,
"Babeş-Bolyai" University, Cluj-Napoca

Reviewers:

Professor Andreea Ioana Stănilă, MSc, PhD
Faculty of Chemistry and Chemical Engineering,
University of Agricultural Sciences and Veterinary Medicine in Cluj-Napoca

Professor Mircea-Nicolae Palamaru, MSc, PhD
Faculty of Chemistry and Chemical Engineering,
"Alexandru Ioan Cuza" University in Iassy

Professor Adrian Pătruţ, MSc, PhD
Faculty of Chemistry and Chemical Engineering,
"Babeş-Bolyai" University, Cluj-Napoca

TABLE OF CONTENTS

SYNOPSIS

50 polyoxometalates (POMs) including 7 original compounds, 40 synthesized based on literature methodology and 3 commercially-available products were characterized in terms of physico-chemical properties via atomic absorption, UV-Vis, FT-IR, ESR and NMR spectroscopy, thermal analysis and transmission electron microscopy. Hypoglycemic, antibacterial and antitumor biological activities were studied. Based on our *in vivo* and *in vitro* studies, we concluded that the two W-POMs we tested in the treatment of streptozotocin-induced diabetic rats and for stimulating mesenchymal stem cells differentiation into insulin-producing cells achieved their hypoglycemiant effects by two concomitant mechanisms: they prevented the apoptosis of pancreatic β-cells and stimulated differentiation of pancreatic resident stem cells into new insulin-producing cells. The antibacterial activities of 37 POMs were tested on Gram-positive and negative bacteria vs. nine antibiotics and 10 POMs presented significant antibacterial activity at the concentrations tested. Antitumor activities of 9 Mo-POMs and 18 W-POMs were investigated *in vitro* on HUVEC and HeLa cell lines. All Mo-POMs and 9 W-POMs initiating apoptosis due to their cytotoxic effects on both cell lines, 7 W-POMs had no effect on cell proliferation, while 2 compounds stimulated it.

KEY WORDS:

polyoxometalates, tungsten, vanadium, molibden, synthesis, antibacterian activity, diabetes, pancreatic beta-cells, stem cells, antitumoral activity

INTRODUCTION

Developing innovative nanocompounds exhibiting effective antiviral, antibacterial and antitumor effects can provide an alternative approach to conventional treatments of cancer and infectious diseases, some of the most serious threats to human health. Due to their unique physical and chemical properties, these inorganic metal oxide clusters with high negative charge modeled through derivatization are suitable for the synthesis of nanocomposites with targeted biological properties. Polyoxometalates are considered intelligent nanomaterials as these oligomeric aggregates are formed by "green" self-assembly processes, the cheapest in the industry.

Their biomedical applications have been extensively developed in the last three decades, based on the particularity that modeling any of the molecular property of nanoPOMs (slight changes in polarity, redox potential, surface charge distribution, shape or pH) can decisively reconfigure their ability to specifically recognize targeted macromolecules (proteins, DNA, RNA etc.) of various normal/pathological biological substrates and the reactivity of such macromolecules under the influence of nanoPOMs. Such complex nano-manipulation possibilities opened by newly available technologies marks this area as one of the most active in the scientific and technological research.

These perspectives provide the foundation of this thesis.

The results presented herein were obtained as follows:

- synthesis and various physico-chemical characterization of some polyoxometalates were performed in the Department of Chemistry - Inorganic Chemistry within the Faculty of Chemistry and Chemical Engineering of the "Babes-Bolyai" University, Cluj-Napoca;
- physico-chemical characterization of polyoxometalates was conducted in the Discipline of Physical Chemistry and Discipline of General and Inorganic Chemistry, Faculty of Pharmacy, "Iuliu Haţieganu" University of Medicine and Pharmacy, Cluj-Napoca, in co-operation with the "Raluca Ripan" Institute of Chemistry, Cluj-Napoca;
- characterization of the relationship between molecular structure and biological activity was a joint effort involving several research units in Cluj-Napoca. As such: determination of the antibacterial activity of the synthesized compounds implied the cooperation with three disciplines within the Faculty of Veterinary Medicine, University of Agricultural Sciences and Veterinary Medicine in Cluj-Napoca, i.e. the Microbiology, Immunology and Epidemiology

Discipline, the Reproduction, Obstetrics and Reproduction Pathology Discipline and the Infectious Diseases and Preventive Medicine Discipline;

- determination of the anti-tumor activity (in vitro study) was performed in cooperation with the Laboratory of Radiobiology and Tumor Biology, "Prof. Dr. Ion Chiricuţă" Oncology Institute, Cluj-Napoca;
- determination of the hypoglycemic **activity** of two polyoxometalates (in vivo study) was performed in the Electron Microscopy Laboratory of the Cell and Molecular Biology Discipline, Faculty of Medicine, "Iuliu Haţieganu" University of Medicine and Pharmacy, with the participation of Assistant lecturer Modeste Wankeu-Nya, MSc, PhD, from the Department of Animal Organisms Biology, Faculty of Science, University of Douala, Cameroon;
- determination of the hypoglycemic activity of two polyoxometalates (in vitro study) was performed in cooperation with the Laboratory of Radiobiology and Tumor Biology, "Prof. Dr. Ion Chiricuţă" Oncology Institute, Cluj-Napoca;

The results presented in this work were published, communicated or are pending to be published.

MOTIVES IN CHOOSING THIS RESEARCH THEME

This PhD thesis contributes in providing new knowledge in the dynamic field of nanocompounds, a topical national and international research theme in view of their exponentially growing number of new applications in medicine, energy, catalysis, materials science etc. Biologically active nanocompounds are needed for providing new and relatively inexpensive inorganic drug formulations that would improve the quality of life. Our efforts included theoretical contributions in understanding the mechanisms leading to the self-assembling of certain polyoxometalates presenting biological activity, synthesis of such huge archetypal complexes (including the synthesis of 7 brand-new compounds), and in detailed analyses of the relationship between the chemical structure of certain classes of polyoxometalates and their biological activity.

OBJECTIVES

The objectives of this research were:

1. Synthesis of several types of polyoxometalates and clusters, including:
    - polyoxometalates presenting saturated structures
    - polyoxometalates presenting lacunary structures
        - POMs presenting mono-lacunary Keggin structures with identical addenda atoms
        - POMs presenting mono-lacunary Keggin structures with mixed addenda atoms
        - POMs presenting tri-lacunary Keggin structures
        - POMs presenting sandwich trilacunary Keggin and pseudo-Keggin structures
        - POMs presenting sandwich trilacunary pseudo-Keggin structures with BiW9 blocks
        - POMs presenting Wells-Dawson mono-lacunary structures with mixed addenda atoms
    - clusters with organometallic fragments
    - clusters with f cations
2. Physico-chemical analyses of all synthesized compounds, including:
    - elemental analysis
    - determination of the chemical structure by spectroscopic methods
        - UV-Vis
        - FTIR
        - NMR
    - stability in aqueous solutions at a physiological pH
    - thermogravimetric analysis
3. Establishing the biological activity of the synthesized compounds
    - antibacterial activity
    - anti-tumor activity
    - hypoglycemic activity
4. Establishing relations between chemical structure and biological activity
    - determination of the factors susceptible to optimize synthesis methods
    - determination of derivatization schemes susceptible to elicit a maximum biological response from the targeted biological substrates

PART I. STATE OF THE ART

Chapter 1. Theoretical aspects in the study of polyoxometalates

Polyoxometalates were discovered by Schele in 1727 [1] and later on by Berzelius in 1826. In 1862 Marignac [2] established their chemical composition and in 1934 Keggin determined the structure of the $[X^{n+}M_{12}O_{40}]^{(8-n)-}$compounds (later called the Keggin structure) based on X-ray diffraction [3-5]. A real revolution in structural terms came six decades later, when isolation of single crystals from molybdenum blue solutions revealed the huge polioxometalate wheel structure encapsulating 158 Mo atoms and the high symmetry of the complex and its surprising solubility were observed. The discovery dramatically changed state of the art data, opening new fields in nanochemistry and nanomaterials.

Polyoxometalates are coordinate covalent compounds of several polyoxoanions usually of group 5 or 6 transition metals in their high oxidation states, mainly molybdenum(VI), tungsten(VI), vanadium(V), niobium(V) or tantalum(V), linked together by shared oxygen atoms to form large 3-dimensional frameworks that may include one or more hetero-atoms such as phosphorus or silicon [6,9].

A first classification divides them into iso-polyoxometalates and hetero-polyoxometalates pending on the absence or presence of hetero-atoms in their composition. While iso-polyoxometalates are based on the Lindqvist structure ($[M_6O_{19}]^{n-}$), hetero-polyoxometalates exhibit a larger variation. Following Keggin's discovery, several other types of hetero-polyoxometalates presenting complete or lacunary structures were found. [2,6-8]

A general formula that underpins their structure can be expressed as $\mathbf{[H_aX_xZ_zM_mM_n^*O_yL_lH_h^*]^{p-}}$, where H are ionizable hydrogen atoms, X are primary heteroatoms, Z are secondary heteroatoms, M are first addenda atoms, M* are second addenda atoms; O are oxygen atoms, L are ligands and H* are hydrogen constitutive atoms.[7,8]

Chapter 2. Synthesis and analyses of polyoxometalates: current stage of research

Polyoxometalates' syntheses are complex processes involving molecular reorganization, therefore reaction mechanisms leading to the formation of new compounds are rather difficult to establish. However, several possibilities are well documented, such as the "all-in-one-pot" synthesis or indirect synthesis from other polyoxoanions. A number of parameters need to be strictly controlled, including pH and temperature (vital in generating the self-assembling mechanism), reflux, hydrothermal

or ambiental conditions, the type and concentration of oxigenic anions, the presence/absence and concentration of certain heteroatoms or addenda atoms, ionic strength, the presence of reducing agents or the composition and organic/inorganic nature of the solvent(s).[2, 23]

The "all-in-one-pot" synthesis takes place in a single of few step(s) and consists in decreasing (for W or Mo) or increasing (for V) the pH of an aqueous solution of oxometalates, thus increasing the nuclearity of the oxoanion fragments. Incorporation of heteroatoms, lacunary fragments or ligands contribute significantly to changes in the structure and architecture of final synthesis products. No intermediate separation/purification steps are needed.

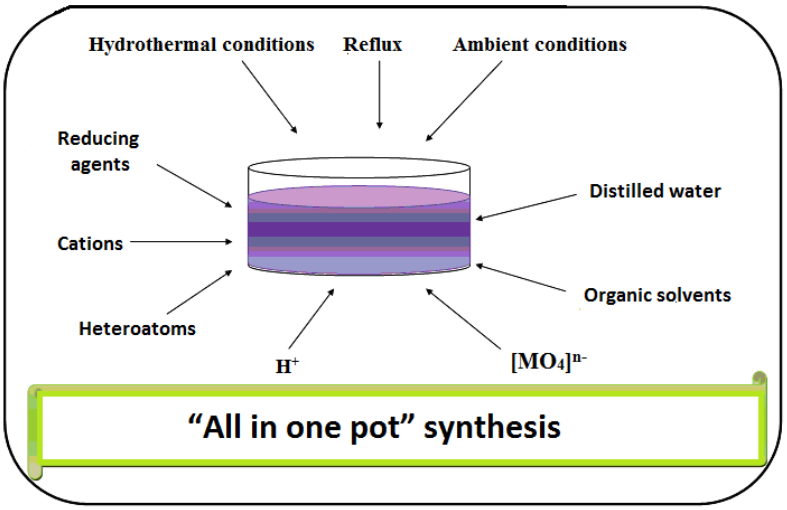

Fig. I.2.1. The *„all in one-pot"* synthesis [modified from 23].

The most frequently used methods to determine optimal conditions for the aqueous synthesis of polyoxometalates and characterize various chemical species in terms of molecular structure are the colorimetric, spectrophotometric, conductometric and polarographic methods.

The conductometric (or potentiometric) method is used in the aqueous synthesis of colorless reactants. According to the electrical quantity that is measured, potentiometric titrations involve the measurement of the potential difference between two electrodes of a cell, while conductometric titrations determine the electrical conductance or resistance.

Polarography is a voltammetric measurement whose response is determined by combined diffusion/convection mass transport. Polarography and cyclic voltammetry are based on the polyoxometalates' reversible reduction which can influence optimal conditions in forming chemical species, and this method was successfully used in discovering new isomers or heteropolyanion fragments. [8]

Spectroscopy (study of the interaction between matter and electromagnetic radiation) is widely used in determining various physical properties. UV-Vis (the ultraviolet and visible spectroscopy), microwave spectroscopy, IR spectroscopy, FT-IR (Fourier transform infrared spectroscopy), Raman spectroscopy, SERS (surface enhanced Raman spectroscopy), SERRS, SPR (surface plasmon resonance spectroscopy), ERS (electron spin resonance spectroscopy), NMR (nuclear magnetic resonance spectroscopy) are among the most frequently employed techniques. Other physical investigations include mass spectrometry (FABMS: fast-atom bombardment mass spectroscopy), thermogravimetric analysis or crystallographic studies based on X-ray diffraction [24-31].

Physical and chemical characterization by elemental and thermogravimetric analysis, fluorescence spectroscopy techniques, UV-Vis, NIR, Raman and SERS vibrational spectroscopy, Raman confocal or atomic force microscopy, followed by remodeling (derivatization) and *in vitro* and *in vivo* testing, is the key to enhance polyoxometalates' biological effects [53-55].

Chapter 3. Polyoxometalates' applications and practical relevance

Because of their structural diversity and of the many types of possible interactions, polyoxometalates show specific physico-chemical properties that provide them with a large versatility.

In analytical chemistry polyoxometalates have been widely used for the detection, separation and dosing of dozens of elements. The presence of multiple drugs in biological samples is determined using polyoxometalates. They are also used in staining different tissue preparations.

Possible applications: analytical reagents, pigments, dyes, tonner ink, catalysis, photo/electro-catalysis, photovoltaic cells, opto-electronic devices, biology and medicine. In this chapter a brief description of the POMs' applications based on their molecular interaction is provided (see fig. I.3.2)

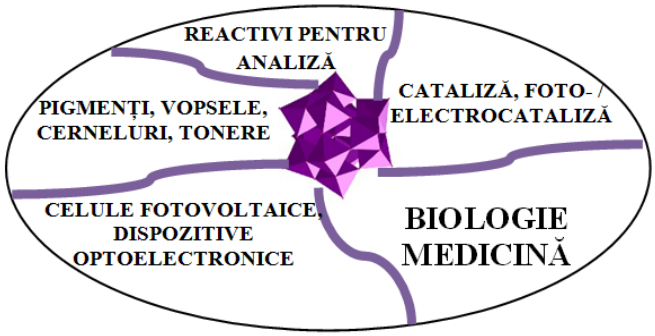

Fig. I.3.2. Applications of polyoxometalates

Chapter 4. Polyoxometalates: biologically active nanocompounds presenting multiple medical applications

In regard of their possible medical applications, heteropolyoxometalates are more efficient than isopolyoxometalates in terms of biological activity because of their versatility in allowing structural changes during syntheses processes. Biological compatibility is their toughest challenge, as being inorganic substances is a major disadvantage. However, changes in their molecular properties (redox potential, electrical charge distribution, acidity), functionalization, kinetically controlled selective assembly, stabilization in aqueous media and derivatization may enhance their compatibility with the biological environment at a physiological pH [62]. Their most important biological actions with possible applications in medicine (antibacterial, antiviral and antitumor activity) were highlighted during our applied research studies.

Although several studies clearly demonstrated the ability of various heteropolyoxoanions to penetrate cell membranes, the complex molecular penetration mechanism is still enigmatic.

The antibacterial activity of the polyoxometalates was demonstrated on a large number of strains resistant to antibiotic action. Various studies (Tajima and Yamase in particular) reported certain antibacterial activities of polyoxometalates combined with β-lactamics (first efficient antibiotics) observed on the likes of Escherichia coli, Methicillin-resistant Staphylococcus aureus (MRSA), Vancomycin-resistant Staphylococcus aureus (VRSA), Helicobacter pylori or Bacillus subtilis [72-80]. More recently heteropolyoxometalates were recently employed in fighting the prionic diseases.[84]

Reported since 1971, the antiviral activity of the polyoxometalates was observed on viruses such as MLSV (murine leukemia sarcoma virus), VSV (vesicular stomatitis virus), polio virus, rubella virus, RLV (Rauscher leukemia virus), RV (Rabies virus), Rhabdovirus or EBV (EBV – Epstein-Barr virus) [94-102]. Promissing results give polyoxometalates a fighting chance against HIV, HBV, hepatic (liver) or herpetic viruses (HSV-1, HSV-2, HCMV), and against some aggressive flu viruses as well [102,103]. Several studies indicated that the reverse transcriptase of the HIV-1 virus is selectively inhibited by certain polyoxometalates [100]. As they do not directly interact with viruses in the host organisms, polyoxometalates' main action is antiviral, not virucidal. Their action depends on size, charge, structure, polyoxoanions and counter-anions' composition, as well as the virus type (DNA, RNA) or cell lines on which the polyoxometalates' activity was tested [72].

Molecular interactions between Keggin polyoxoanions and bovine hemoglobin proved the potency of the anticoagulant action of polyoxometalates as they strongly inhibited protein tyrosine phosphatase. Chronometering the dynamics of human blood coagulation processes confirmed that Keggin saturated polyoxometalates exhibit anticoagulant activity mainly based on the polyoxoanions' degree of hydration [123-125].

Data on the anticancer mechanism exerted by polyoxometalates are not well understood, the only in vivo human study in 1965 reporting succesful blockage of urinary blade carcinoma evolution under treatment with tungsten and molybdenic acids combined with coffein [106]. In vitro studies on malignant cells lines revealed that the polyoxometalates' antitumor activity surpases that of certain cytostatic drugs [107-109]. It was observed that the polyoxoanion influences antitumor activity, while the cation determines its biodisponibility (solubility). By activating the apoptotic pathway in reducing mitochondrial activity, polyoxometalates inhibit ATP generation based on a redox reaction, as proposed by Yamase. Polyoxometalates were found to present great specificity against CK2 protein-kinase, a global anti-apoptotic agent [110-115].

In the 80's a number of in vivo experiments using streptozotocin or alloxan established the hypoglycemic activity of certain vanadium-based compounds, but indicated high toxicity levels [149-152]. Vanadyl sulfate is used as a nutrition supplement and tested since 2000 in clinical trials with promising results and no significant side effects, but further studies concentrated on tungsten and molybdenum compounds to reduce toxicity while enhancing the hypoglycemic activity [145-148]. It has been determined that vanadium enhances insulin action, but actual mechanisms are still under debate [149-152]. Latest research considered using Dawson polyoxometalates presenting both vanadium and tungsten.

II. PERSONAL CONTRIBUTIONS

Chapter 1. Synthesis and physico-chemical analyses of polyoxometalates presenting saturated and lacunary structures

51 polyoxometalates including 7 original compounds, 41 synthesized based on literature methodology and 3 commercially-available products were characterized in terms of physico-chemical properties.

The newly synthesised 7 polyoxomethalates are:

1. $(NH_4)_4[NBu_4]_5[Na(BuSn)_3Sb_9W_{21}O_{86}]\cdot 17H_2O$ (POM 2 D=POM BI-28)

2. $Na_8[La_2(H_2O)_6(Bi_2W_{20}O_{70})]\cdot 37H_2O$ (POM T-8)

3. $Na_{15}[(CeO)_3(OH_2)_2(BiW_9O_{33})_2]\cdot 45H_2O$ (POM T-10)

4. $K_6[SiVW_{11}O_{40}]\cdot 12H_2O$ (POM BI-30)

5. $K_6[Si(VO)Mo_2W_9O_{39}]\cdot 11H_2O$ (POM BI-7)

6. $Na_5[Fe(H_2O)GeW_{11}O_{39}]\cdot 26H_2O$ (POM BI-24a,b=POM T-26)

7. $Na_{14}[Mn_3(H_2O)_3(SiW_9O_{34})_2]\cdot 25H_2O$ (POM BI-27=POM T-11).

Synthesis and physicochemical characterization of $(NH_4)_4[NBu_4]_5[Na(BuSn)_3Sb_9W_{21}O_{86}]\cdot 17H_2O$.

The **$(NH_4)_4[NBu_4]_5[Na(BuSn)_3Sb_9W_{21}O_{86}]\cdot 17H_2O$** complex (POM2D=POM BI-28) with an original formula proposed here, specific for the synthesis of a larger polyoxometalate derived with organometallic fragments, was newly prepared and characterized as follows:

To a 3.3 mmol solution made of 0.66 mL $C_4H_9SnCl_3$ in 50mL bidistilled and deionized water, powdered $(NH_4)_{17}Na[NaSb_9W_{21}O_{86}]\cdot 14H_2O$ (6.94 g, 1 mmol) was added quickly and under continuous stirring at 50-60ºC. Within a few seconds, most of 21-tungsto-9-antimonate cryptate dissolved and the solution became clear; its final pH was 5.0. Traces of unreacted tungstoantimonate were filtered out after 10 minutes, and $(NBu_4)Br$ (1 g, 2.7 mmol) was subsequently added in small amounts to the filtrate and a white precipitate was obtained. The precipitate was then collected on a fine glass frit, dried under a water aspirator vacuum system for 1h, washed with saturated $(NBu_4)Br$ solution and dried overnight under vacuum to give a yield of 3.60 g (39%). A white powder of this solid compound was obtained by the method of vapor diffusion with ethanol; yield 2.94 g (31%) [80].

The elemental analysis of the POM2 was consistent with our proposed formula: $(NH_4)_4(NBu_4)_5[Na(BuSn)_3Sb_9W_{21}O_{86}]\cdot 17H_2O$. Calculated: for $C_{92}H_{257}N_9NaSb_9Sn_3W_{21}O_{103}$ (M=8473.62): C, 13.04; H, 3.06; N, 1.49; Na, 0.27; Sb, 12.93; Sn, 4.20; W, 45.56; H_2O, 3.61. Found: C, 13.06; H, 3.10; N, 1.54; Na, 0.28; Sb, 12.94; Sn, 4.35; W, 45.61; H_2O, 3.64.

Thermal analysis of the POM2 nanocompound revealed the presence of 17 molecules of crystal (lattice) water. The most interesting aspect of our study was the interaction between $BuSn^{3+}$ and $[NaSb_9W_{21}O_{86}]^{18-}$ by a cyclic self-assembly of the $(B\text{-}\beta\text{-}SbW_7O_{24})^{3-}$ anions linked by two Sb_3O_7 external fragments in which $[Na(BuSn)_3Sb_9W_{21}O_{86}]^{9-}$ polyoxometalate complexes were formed. The product of reaction between $[NaSb_9W_{21}O_{86}]^{18-}$ and $BuSn^{3+}$ ions in aqueous solution, isolated as the mixed ammonium and tetra-butyl ammonium salt, proved to be $(NH_4)_4(NBu_4)_5[Na(BuSn)_3Sb_9W_{21}O_{86}]\cdot 17H_2O$ in which one B-β-$[NaSb_9W_{21}O_{86}]^{18-}$ anion was linked by O-Sn-O bridges. The polyoxotungstate anion consisted of a B-β-$[NaSb_9W_{21}O_{86}]$ fragment (L2), which linked three $BuSn^{3+}$ fragments in three pentavacant ligands by five terminal oxygens, and all tin ions had one terminal n-butyl, resulting in octahedral coordination geometry. This anion (POM2) was the first one derived from B-β-$[NaSb_9W_{21}O_{86}]^{18-}$ anion and butyltin cations. Tungstoantimonate (III) anion $[NaSb_9W_{21}O_{86}]^{18-}$ contained three $\{SbW_7O_{24}\}$ groups linked to a central core of two $\{Sb_3O_7\}$ groups, encapsulating a sodium cation, forming the central active site. The $\{SbW_7O_{24}\}$ units were pentavacant lacunary derivatives of the hypothetical Keggin $\{\beta\text{-}SbW_{12}\}$ anion, by removal of five WO_6 octahedra (a W_3O_{13} triplet and one octahedron from two different triplets), forming another six sites disposed two towards the three $\{SbW_7O_{24}\}$ subunits. Two adjacent lacunary sites on each $\{SbW_7O_{24}\}$ group could be occupied with one or two transition cations in order to form nanocomplexes (see figura II.2.11) [81,82].

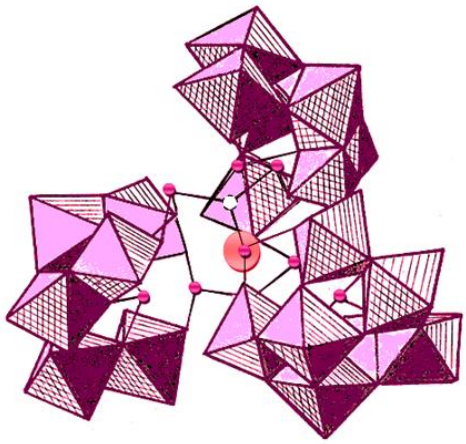

Fig. II.2.11 Structure of the B-β-$[NaSb_9W_{21}O_{86}]^{18-}$ polyanion, poliedric representation of the three $\{SbW_7\}$ fragments: WO_6 polihedre in purple, Oxigen atom – white ball, Sb atoms - pinkballs, large orange ball - Na^+ [modified after Zhang, 1995].

Thermal analyses revealed the following: The first important process was the weight loss, accompanied by two endothermal effects at temperatures in the range of 40-240°C. This corresponded to

the elimination of 17 (3.61%) water molecules, with loss of the lattice water in two steps. The next important process observed at 200-350°C related to changes in the polyanionic architecture, compared with other polyoxometalates. Above 380°C, after combustion of organic components, inorganic residue exhibited some minor exothermal effects probably due to a polymorphic transformation.

The **UV electronic spectra** of HPA-23 as L2 and of POM2 (POM BI-28) exhibited two charge-transfer bands, also observed for L1 and POM1, characteristic for polyoxometalate structures.

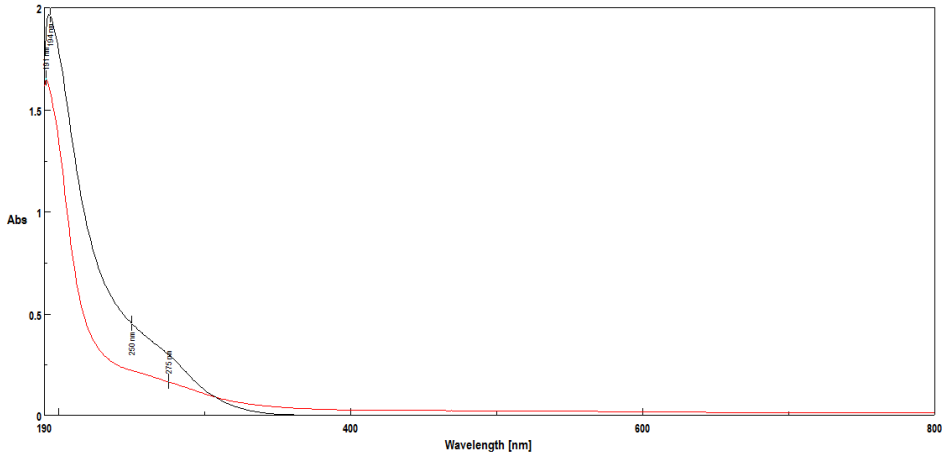

Fig. II.2.2. UV spectra of L2 (in black) and POM2=POM BI-28 (in red).

Table 1. UV spectra chemical shift (nm/cm^{-1}).

	ν_2 (W=O$_t$)	ν_1 (W-O$_{c,e}$-W)
L2-HPA23	194 nm/51546 cm^{-1}	250 nm/40000 cm^{-1}
POM2	191 nm/52356 cm^{-1}	275 nm/36363 cm^{-1}

O_i is a internal oxygen which links Sb and W atoms; $O_{c,e}$ are the oxygen atoms which connect corner and edge sharing WO_6 octahedra; and O_t is a terminal oxygen.

The UV spectra of L2 and POM2 were very similar, providing evidence that the charge transfer inside the polyoxotungstate structure was not significantly affected by coordination. The more intense band, corresponding to the $p_\pi(O_t) \rightarrow d_\pi(W)$ transition, was centered at 51 546 cm^{-1}(194 nm) in L2 and at 52 356 cm^{-1} (191 nm) in POM2 (O_t is a terminal oxygen). This was in agreement with the coordination of metallic ions by the terminal oxygen atoms of the pentavacant ligand L2. The broader band centered at 40 000 cm^{-1} (250 nm) in the L2 spectrum belonged to the $p_\pi(O_{c,e}) \rightarrow d_{\pi*}(W)$ charge transfer transition in the tricentric bands W-O$_{c,e}$-W. ($O_{c,e}$ are the oxygen atoms which connect corner and edge sharing octahedra.) This band was much more shifted toward lower energies in the case of POM2 at 36 363 cm^{-1} (275 nm). This finding was in agreement with the intensification of inequivalence in these bonds, also showing a symmetry decrease originating from distortion of the corresponding WO_6 octahedra.

Vibrational spectra. All of the prepared POMs and their corresponding ligands have characteristic IR spectral bands in the range 700-1000 cm^{-1} [83]. FT-IR spectra of polyoxometalates generally exhibited contributions of the polyoxoanion framework [84-87]. These bands were shifted by comparison with lacunary polyoxometalates because of the structural changes caused by the coordination of the vanadyl $(VO)^{2+}$ ions in POM1 or organometallic (butyltin) fragments in POM2. In this work, the FT-IR spectrum of new $(NH_4)_4(NBu_4)_5[Na(BuSn)_3Sb_9W_{21}O_{86}]\cdot 17H_2O$ (POM2) nanocomplex, when compared to the spectrum of $(NH_4)_{17}Na[NaSb_9W_{21}O_{86}]\cdot 14H_2O$ (L2) (**Figure** II.2.3), information was provided concerning the coordination of $BuSn^{3+}$ ions by the different type of oxygen atoms from POM2. As was predicted, L2 and POM2 displayed the IR spectral bands characteristic of polyoxometalates. (Table II.2.2).

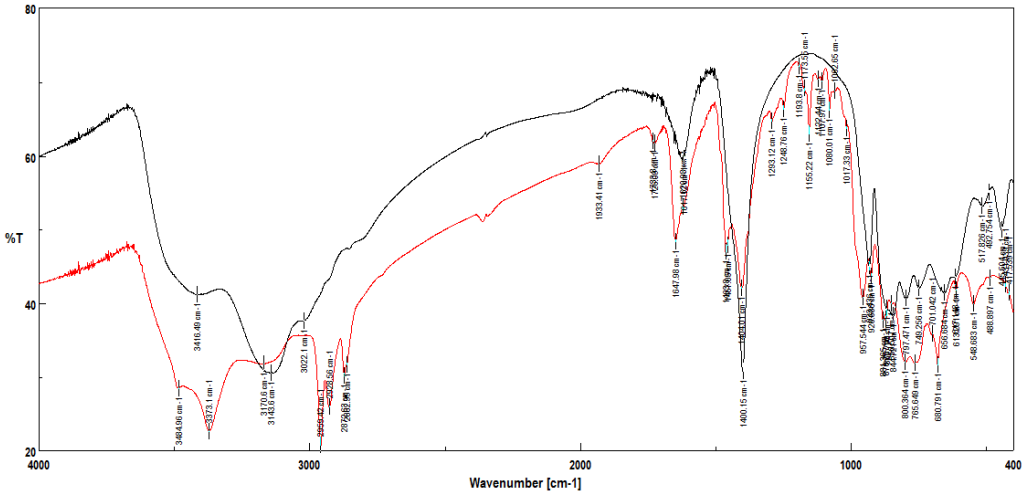

Figure II.2.3. FT-IR spectra of L2 (in black) and POM2 (in red).

Table II.2.2. Vibrational frequencies (cm^{-1}) from FT-IR spectra of L2 and POM2.

Assignment	L2	POM2
ν_{as}(W=O_t)	933s	958s, 927m
ν_{as}(W-O_c-W)	870s, 845s	881s, 871s, 851s
ν_{as}(W-O_e-W)	797vs, 749vs	800vs, 766vs
ν_{as}(Sb-O_i)	657s, 518w	681s, 613m, 549s
ν_{as}(Sn-O)	-	681s, 549s
ν_{as}(C-Sn-O)	-	681s, 549s
ν_{as}(C-Sn)	-	489m, 418m
ν(C-N)	-	1293m, 701 sh
ν_{as}(O-H) from H_2O	3416s	3485s, 3373vs
ν_{as}(N-H) from NH_4^+	3144vs, 3022sh	3171m, br
δ(W-O-W)	493w	489vw
δ(Sb-O)	446m	431w
δ(O-H) from H_2O	1617m	1648m, 1621sh
δ(N-H) from NH_4^+	1400vs	1404s
ν_{as}(C-H) from butyl	-	1000-1300, 1700-1950, >2800

NMR spectra. The ^{1}H- and ^{13}C-NMR spectra indicated the equivalence of all of the butyltin groups. Unfortunately, we have not been able to obtain high quality spectra to date. This may be due to the very low solubility of compounds in the used solvent ($CDCl_3$) [94]. However, the ^{1}H- and ^{13}C-NMR spectra of the *n*-$BuSnCl_3$ and POM2 were quite similar and exhibited the expected resonances. They also showed four signals typical of the butyl group; however, these signals (in POM2) were relative shifted as compared to *n*-$BuSnCl_3$ (as the reference standard) [95]. These values are shown in Table II.2.3.

Table II.2.3. The chemical shifts (δ, ppm) of resonance signals from ^{1}H-NMR and ^{13}C-NMR spectra of n-$BuSnCl_3$ and POM2.

^{1}H-NMR spectra	**n-$BuSnCl_3$**	**POM2**
C$\underline{H}_2$,α	2.41	2.05
C$\underline{H}_2$,β	1.90	1.85
C$\underline{H}_2$,γ	1.50	1.42
C$\underline{H}_3$,δ	0.98	0.88
^{13}C-NMR spectra	**n-$BuSnCl_3$**	**POM2**
$\underline{C}H_2$,α	33.54	32.04
$\underline{C}H_2$,β	26.93	27.83
$\underline{C}H_2$,γ	25.74	26.22
$\underline{C}H_3$,δ	13.44	13.51

- $Sn-{}^{\alpha}CH_2-{}^{\beta}CH_2-{}^{\gamma}CH_2-{}^{\delta}CH_3$

Comparison of the ^{1}H-NMR spectra of $(NH_4)_4(NBu_4)_5[Na(BuSn)_3Sb_9W_{21}O_{86}]\cdot 17H_2O$ and free butyltin-trichloride indicated that they were nearly identical, which may be due either to the weak binding constant or to the swift exchange of butyltin fragments on the NMR time scale. In addition, due to the diamagnetic character of W(VI), the complexation shifts were slightly different as expected [95,96]. For POM2, the ^{1}H-NMR chemical shifts (δ, ppm) of resonance signals were centered at 2.05 (multiplet, C$\underline{H}_2$,α), 1.85 (quintet, C$\underline{H}_2$,β), 1.42 (sextuplet, C$\underline{H}_2$,γ), and 0.88 (triplet, C$\underline{H}_3$,δ), relative to *n*-$BuSnCl_3$ (2.41; 1.90; 1.50 and 0.98 ppm) in the aliphatic region. The ^{1}H-NMR spectrum was not very well resolved, and yet all resonances could be unambiguously assigned; nevertheless, the allure spectrum suggested the existence of a single chemical species, namely POM2.

The ^{13}C-NMR chemical shift of carbon signals showed a correlation with the nature of the butyltin group and with the new C-Sn-O bound [95] as in the POM2 structure. The ^{13}C-NMR resonance signals in the POM2 spectra were slightly shifted at 32.04 ($\underline{C}H_2$,α), 27.83 ($\underline{C}H_2$,β), 26.22 ($\underline{C}H_2$,γ), and 13.51 ($\underline{C}H_3$,δ) ppm compared to the free *n*-$BuSnCl_3$ (33.54; 26.93; 25.74 and 13.44 ppm), consistent with the coordination of tin atoms attached to the terminal oxygen atoms tied to tungsten (VI) atoms.

The ^{13}C-NMR spectrum of POM2 in $CDCl_3$ displayed the expected resonances for the aliphatic carbon atoms and showed four clean lines, confirming the purity and the single-product nature.

Synthesis and physicochemical characterization of $Na_8[La_2(H_2O)_6(Bi_2W_{20}O_{70})]\cdot 37H_2O$ (POMT-8)

This synthesis was carried out in aqueous solution by mixing the ingredients in acid medium, according to stoichimetry of the chemical reactions taking place. The compound was further characterized by several physical and chemical methods.

Two BiW_9 subunits of the heteropolyoxoanions formed during synthesis capture two WO_6 octahedron and two La^{3+} cations in a sandwich structure, the proposed resulting compound presenting a Bi_2W_{20} structure with a C2h symmetry (including an inversion center) being shown in Figure II.2.15

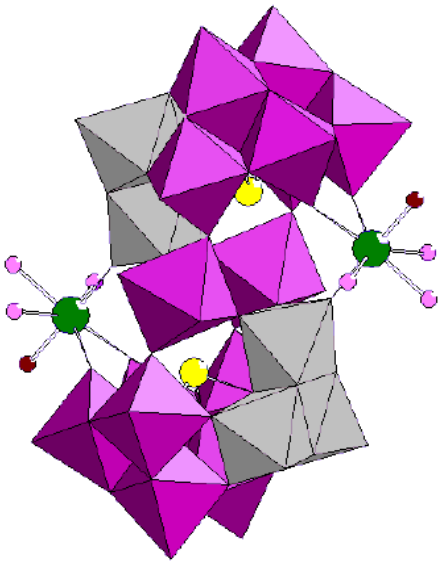

Fig. II.2.15. Polyhedral representation of the $[La_2(H_2O)_6(Bi_2W_{20}O_{70})]_8^-$ polyoxoanion (in purple: WO_6 octaedra; in gray: WO_6 octaedra rotated 60º; green balls: La^{3+} ions; yellow balls: Bi heteroatoms of the BiO_4 tetrahedra; pink balls: coordinated water molecules; red balls: oxygen atoms).

The lanthanide ions are thus heptacoordinated in a pentagonal bipyramidal geometry. These structures can self-assemble in dimers and can form monodimensional layers.

Synthesis and physicochemical characterization of $Na_{15}[(CeO)_3(H_2O)_2(BiW_9O_{33})_2]\cdot 48H_2O$

This synthesis was carried out in aqueous solution by mixing the ingredients in acid medium, according to stoichimetry of the chemical reactions taking place, in a modified version of the method

presented by Gouzerh în 2002.The compound was further characterized by several physical and chemical methods.

Sandwich structures with f metal ions incorporated in their structure have been described by Knoth [21]. For this newly synthesized compound we propose a $Na_{15}[(CeO)_3(H_2O)_2(BiW_9O_{33})_2]\cdot 48H_2O$ structure, as shown in Figure II.2.19.

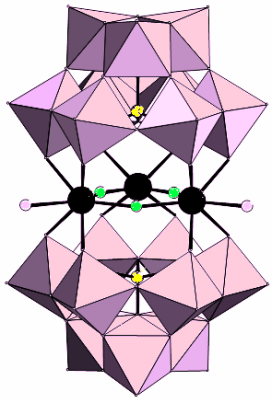

Figure II.2.19. Polyhedral representation of the $Na_{15}[(CeO)_3(H_2O)_2(BiW_9O_{33})_2]\cdot 48H_2O$ polyoxometalate structure (in purple: WO_6 octaedra; black balls: Ce^{3+} ions; yellow balls: Bi heteroatoms of the sandwich structure; green balls: oxygen atoms; pink balls: water molecules).

Chapter 3. Biological activity of the synthesized polyoxometalates

3.1 The hypoglycemic activity of two polyoxometalates - in vitro and in vivo studies

Introduction

Several groups of researchers, including one led by Nomiya, has characterized certain molecules polyoxometalates as insulin-mimetic and having hypoglycemic activity [153]. The study presents the results of investigations concerning two heteropolioxowolframaţi hypoglycemic activity were not investigated in this perspective, POM1 = $K_{11}H[(VO)_3(SbW_9O_{33})_2]\cdot 27H_2O$ = PM-1002 (described for the first time in literature Yamase et al, 2001) and POM 2 = $(NH_4)_4(NBu_4)_5[Na(BuSn)_3Sb_9W_{21}O_{86}]\cdot 17H_2O$ first proposed here in this thesis, proved to have hypoglycaemic activity.

Hypoglicemic effects of the two polyoxometalates have been established in an in vivo study after their oral administration in rats with diabetes induced by STZ (streptozotocin). In order to elucidate the molecular mechanism of action of polyoxometalate, in vitro experiments showed two POMs ability to stimulate the differentiation of stem cells into insulin-producing cells and secreting.

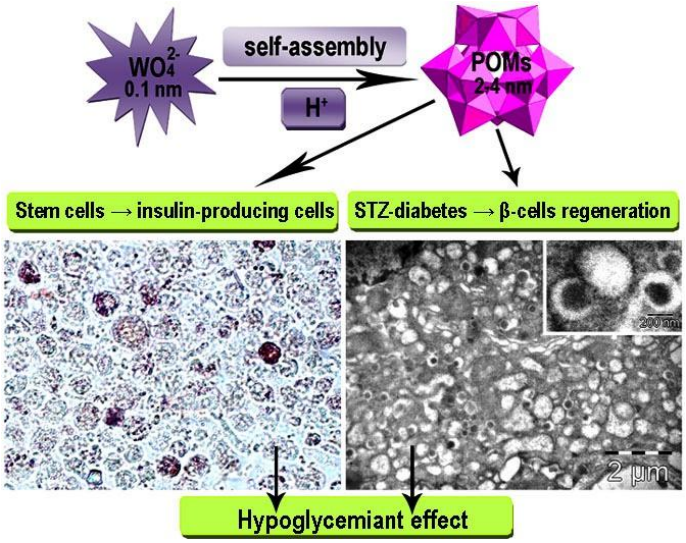

Fig. II.3.1.1. Hypoglicemic effects of the polyoxometalates

Materials and methods

In vivo study

We used male Wistar rats in which diabetes was induced with STZ (50 mg/kg b.w.) intraperitoneally injected in a single dose (Wankeu-Nya et al., 2013). Blood drop collected by venipuncture from each rat were analyzed with Accu-Chek®Active glucose meter (F. Hoffmann, La Roche Diagnostics Ltd.). Glycemia levels higher than 200 mg/dL recorded in all STZ injected rats were considered as indicative for diabetes.

Four control groups were established: healthy control group treated with POM1, POM2 and bidistilled water and two diabetic groups treated with POM1 and POM2. In all groups treated with POMs, the daily dosages (as 1 mg/mL solutions in Millipore water) were up to a cumulative dose of 4 mg/kg b.w. at the end of the 3 weeks of treatment. The blood glucose was monitored at 14 and 21 days respectively – when the rats were killed under general anesthesia.

Distribution and ultrastructural characteristics of the secretory vesicles of endocrine pancreas β cells and insulin-producing cells, as well as the hepatotoxicity assessment as induced by POMs administration, were determined following the transmission electron microscopy (TEM) standardized analytical protocol JEOL JEM 1010 (JEOL Ltd., Tokyo, Japan). Secretory vesicle diameters of β cells and their inside electron-dense granules were measured using the Cell^D morphometry software (Olympus Soft Imaging Solutions GmbH, Münster, Germany).

***In vitro* study**

Three cell lines were used in this study: human bone marrow adult mesenchymal stem cells (M-MSCs), human umbilical vein endothelial cells (HUVECs) and human amniotic membrane adult mesenchymal stem cells (A-MSCs). M-MSCs and A-MSCs were cultured in standard stem cell medium, while HUVECs were cultured in RPMI-1640 medium.

A-MSCs cells in vitro differentiation into insulin progenitor cells was performed based on the protocol of pancreatic differentiation.

Statistical Analysis

GraphPad Prism 5.00 software (GraphPad Software Inc., La Jolla, USA) was used for the statistical analysis and for the graphical representation of the results. The differences were considered statistically significant at $p<0.05$.

Results and discussion

The size of the two POMs were measured manually using the Cell^D software (6093 measurements for each POM) based on TEM micrographs. Distribution of POMs sizes is shown in Figure II. 3.1.2 .

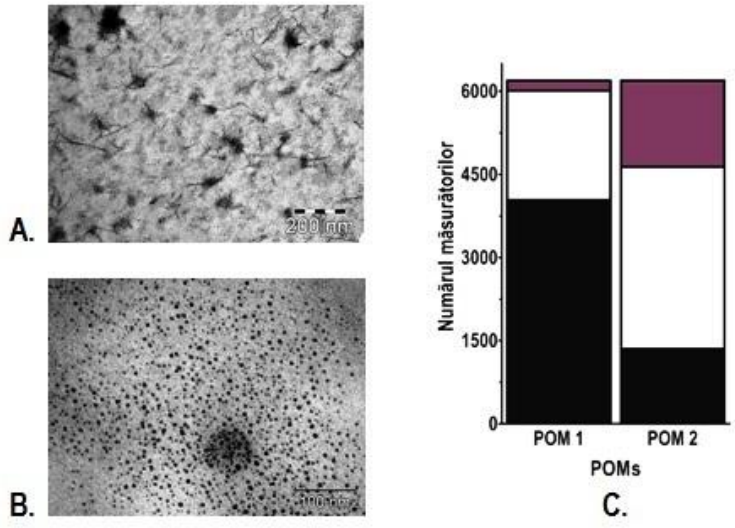

Fig. II.3.1.2. Nanocompounds sizes. A. TEM image of POM1; B. TEM image of POM2; C. POMs' diameter distribution (in black: 2-3 nm, in white: 3-4 nm; in purple: above 4 nm).

Effects of POMs on Body Weight and on Food Intake

No statistical significant effects of the various treatments were observed with regard of food intake during the study. Concerning the body weight of the animals, among the negative controls, only

the HCG group constantly gained weight. The groups treated with POMs underwent an initial increase after 14 days, but with a come back towards the end of the study. On the other hand, in all diabetic groups (positive controls, and two treated with POMs), a continuous loss of weight was observed during the whole experiment.

Hypoglycemic effects of POMs

The blood glucose level had constant values in the three negative control groups during the entire study. In the positive control group, the STZ treatment was followed by a dramatic increase of glycemia due to a high number of affected β-cells by STZ. In the two STZ-diabetic groups treated with POMs, the increase of glycemia was much less pronounced as compared to the positive control group during and at the end of the experiment. There were no statistical significant differences between the levels of blood glucose measured in the day 21 in the diabetic groups treated with POM1 and POM2, but POM1 exerted greater hypoglycemic effects. These aspects are highlighted in figure Fig. II.3.1.3.

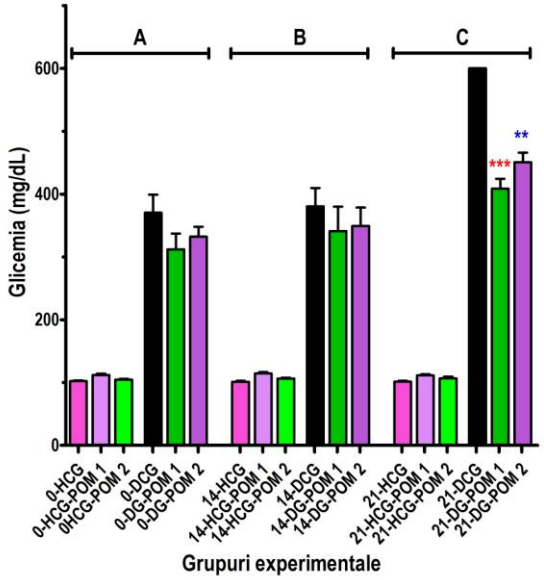

Fig. II.3.1.3. Evolution of blood glucose level during treatment on all experimental groups. A. Day 1; B. Day 14; C. Day 21.

Ultrastructural Aspects of Pancreatic β-Cells

The main ultrastructural characteristic of these cells in the healthy rats group consisted in the presence of many secretory vesicles with a normal distribution within the β cells. It turned out that fixing methods based on glutaraldehyde and osmium tetroxide are responsible for the "classic ultrastructure " of β cells secretory vesicles, exhibiting an electron-dense core (insulin granules) surrounded by a large

gauzy halo. The calculated average diameter of secretory vesicles in the healthy group of rats was 466.67 ± 58.40 nm and the average diameter of the electron-dense core was 264.01 ± 45.29 nm.

In the positive control group many apoptotic β-cells were found in the islets. They were shrunken and detached from the neghbouring cells, presenting irregular nuclei, clumped chromatin granules and dilated perinuclear space, dilated endoplasmic reticulum as well as highly vacuolized cytoplasm. However, other β-cells preserved a generally normal ultrastructure, exhibiting round or oval shaped euchromatinic nuclei, rough endoplasmic reticulum with normal ultrastructural aspect and prominent Golgi apparatus. On the other hand, multilamellar bodies were observed in their cytoplasm and mitochondria were ballooned, with rarefied matrix and disrupted cristae. Most of the secretory vesicles were devoid of the dense core of insulin, or with very small cores. The number of normal-looking secretory vesicles was markedly decreased, most of them having only a thin, bright rim around the insulin core that occupied almost entirely the secretory vesicles. Some of these granules were immature, with reduced electron density. The mean diameter of the secretory vesicles in this group was 273.30±42.88 nm, and for the dense core, a mean diameter of 193.84±101.58 nm was calculated.

The β-cells in the diabeticgroup treated with POM1 displayed oval shaped euchromatinic nuclei with irregular outline, dilated endoplasmic reticulum and prominent Golgi apparatus. Among their secretory vesicles, present in high number, many had normal ultrastructural aspect even though they had smaller diameters. Many other vesicles observed were still devoid of the dense core, and some of the empty vesicles had larger diameters. The mean diameter of the secretory vesicles in this group was 359.88±67.12 nm, and for the dense core, a mean diameter of 124.82±111.29 nm was calculated.

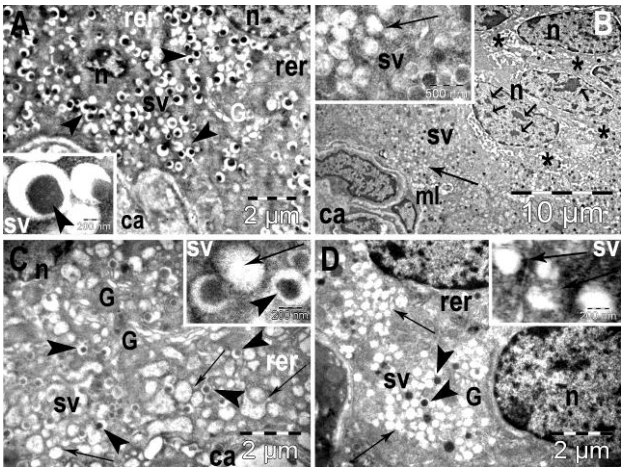

Fig. II.3.1.4. Ultrastructural aspects (TEM micrographs) of pancreatic β cells from different experimental groups. A. healthy rats; B. STZ-induced diabetic rats; C. diabetic rats treated with POM1; D. diabetic rats treated with POM2.

In the group of diabetic rats treated with POM2, rare apoptotic β-cells were found. The intact remained β-cells in this group were in higher number as compared to diabetic control group. The secretory vesicles were present in high number, but the vesicles without the central dense granule of insulin prevailed. Few vesicles contained small dense cores, and even fewer were those with insulin granules of normal sizes. The mean diameter of the secretory vesicles in this group was 178.05±50.03 nm, and for the dense core, a mean diameter of 51.22±71.20 nm was calculated.

An obvious correlation between the average size of secretory vesicles (and their dense cores) and blood glucose levels was observed only when comparing control (healthy and diabetic) groups. In the group treated with POM1, individual β cells exhibited a ultrastructural pattern similar to β cells of healthy controls rats. This indicated a high recovery of their secretory functions, a finding supported by secretory vesicles' larger diameters. In the group of diabetic rats treated with POM2, β cells were more like those in the control group of diabetic rats, an aspect that could explain differencesin the hypoglycemic activity of the two POMs.

Ultrastructural Aspects of Hepatocytes

Examination of TEM micrographs from the negative control group of rats revealed the normal utrastructure of hepatocytes. In the positive control group, important ultrastructural changes of hepatocytes were recorded. Hepatocytes in the diabetic group treated with POM1 displayed oval shaped euchromatinic nuclei with prominent nuleoli and irregular outline, dilated endoplasmic reticulum and numerous heterogeneous secondary lysosomes as main ultrastructural features. The ultrastructure of hepatocytes in the diabetic group treated with POM2 was very similar to that of hepatocytes in group 1, but a lower number of cells appeared to be affected, presenting irregular nuclei and secondary lysosomes in high number. These ultrastructural findings indicated that POMs (in the dosages used here) were able to restore the initially disturbed metabolic activity of hepatocytes in diabetic rats. Our results imply a lack of detectable toxic effect of the two POMs. This has been confirmed by MTT assays performed on cultured cells.

Testing POMs cytotoxicity by MTT assay

HUVEC cells were almost not affected by POM1 – only one of the highest doses proved to have significant inhibitory effect (0.11 mg/mL), but were more sensitive to almost all tested POM2 concentrations. POM1 induced an increased proliferation rate of M-MSCs, changes that were statistically significant at concentrations of 1.12 and 0.56 μg/mL. The effect of POM2 was cytotoxic at high concentrations of 0.2 and 0.11 mg/mL. Concentrations lower than 9 μg/mL also determined a

higher growth of MSCs but not of the same amplitude as POM1. According to these results, concentration of 9 µg/mL for POM1 and POM2 (the highest dose that proved to be non-toxic for M-MSCs) was established for further in vitro differentiation experiments.

Differentiation of stem cells into insulin-producing cells

Differentiation of stem cells in the presence of the two POMs, following differentiation protocols over 4 weeks, included three stages. All tests were performed in triplicate in order to check the reproducibility of the results. Making use of dithizone staining (a specific dye for labeling functional insulin assembled into hexamers), stem cell differentiation was demonstrated in the insulin-producing cells and insulin-secreting. The presence of numerous dithizone positive clusters was noted in all three samples, to a greater extent in A-MSCs treated with POMs.

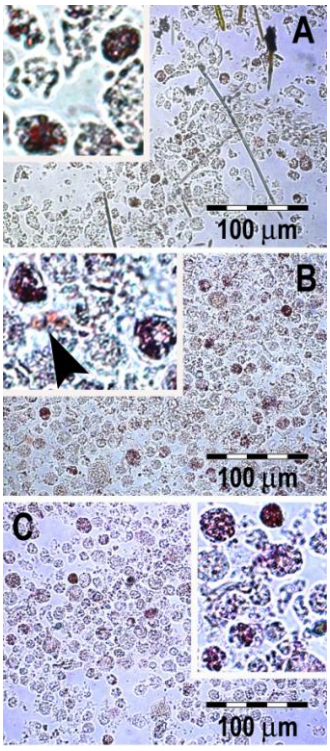

Fig. II.3.1.10. Phase contrast microscopy images: A-MSCs cells differentiate into insulin-producing and insulin-secreting pancreatic cells. AC: A-MSCs differentiated into progenitor pancreatic cells at the end of the differentiation process, after being cultured 6 days in a medium supplemented with glucagon P3 and TGFβ1. A. Control, many dithizono-positive cell clusters; B. In POM1-treated A-MSCs much more dithizono-positive cell clusters were formed; C. POM2 treatment also resulted in a large number of dithizono-positive cells. Details of A-C point out cell clusters containing insulin; in B clusters stained with dithizone are observed, as well as the presence of red-coloured secreted insulin outside the clusters (marked with an arrow).

These results have proved the ability of both POMs to accelerate differentiation of stem cells into insulin-producing cells. Of the two POMs tested POM1 exerted a stronger influence, and the presence of insulin inside the differentiated stem cells was confirmed by the deep red color observed in all cell clusters. In addition, in both POMs the intensity of the red color in some specific cell groups was not so widespread, but near such clusters an amorphous red colored "cloud" was noted. This is even more important than the efficient synthesis of insulin by the stem differentiated cells, as it shows that these cells not only do have the ability to synthesize insulin, but also the ability to secrete the produced insulin.

Conclusions

The two polyoxometalates with average diameters of 2-4 nm presented a significant hypoglycemic activity, subsequent to the oral treatment in an animal model of STZ - induced diabetes. The tris(vanadyl)-substituted tungsto-antimonate(III)-anion (POM1) tested here proved to be stronger in all respects compared to the tris-butyltin-21-tungsto-9-antimonate(III)-anion (POM2). In addition, one of the main benefits emerging from this study was the dose-dependant low toxicity of these nanocompounds. Based on in vivo and in vitro studies, we concluded that the two polyoxometalates tested here have exercised their hypoglycemic effects via two different mechanisms concomitently: they prevented the apoptosis of pancreatic β-cells (and the further reduction in the amount of insulin) and stimulated resident stem cell differentiation into new insulin-producing and insulin-secreting pancreatic cells.

3.2. The antibacterial activity of synthesized polyoxometalates – *in vitro* study

Introduction

One of the most interesting applications of polyoxometalates (POMs) is to establish their antibacterial activities and behavior similar to the antibiotics. Being known antibiotic resistance of bacteria, the discovery of new compounds with strong antibacterial features is an important goal.

In this chapter, we describe the results of the test of antibacterial activities of 37 POMs as follows: 30 compounds in the 1st set compared with amoxicillin (broad-spectrum antibiotic) and 7 in the 2nd set of compounds, pseudo-Keggin polyoxometalates with trilacunare "sandwich" structure (having incorporated into their structure the cations of the transition metals) compared with 9 antibiotics.

These compounds have been tested against several strains of Gram-positive and Gram-negative bacteria. Some tested POMs showed certain antibacterial effects, being a possible alternative to used chemotherapeutic agents. The image below summarizes the effects observed.

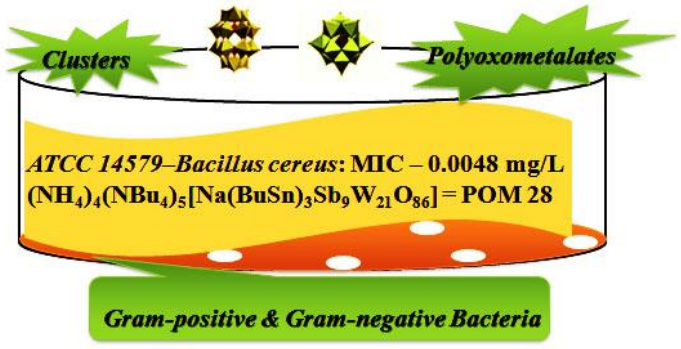

Fig. II.3.2.1. Antibacterial effects of polyoxometalates (graphical abstract).

Materials and methods

Determination of antibacterial activity by difusimetric method

Antibacterial activity of POMs (set I) was determined by difusimetric method, in accordance with the standards imposed by the *Clinical and Laboratory Standards Institute* (2009). The used protocols were adapted for this study and have used five reference strains, two Gram-positives (*Staphylcoccus aureus* and *Bacillus cereus*) and three species of Gram-negative bacteria (*Escherichia coli*, *Salmonella enteritidis* and *Pseudomonas aeruginosa*), purchased from the *American Type Culture Collection* (ATCC, Manassas, VA, USA). The reading of the results was done by measuring the diameter of the zone (area) of inhibition. Highlighting the effects of the POMs was achieved through the method of Gram coloration.

The 2nd set POMs were tested *in vitro* against six reference bacterial strains (two species of Gram-positive bacteria – *S. aureus*, *B. cereus* – and four species of Gram-negative bacteria – *E. coli*, *S. enteritidis*, *P. Aeruginosa*, *S. typhimurium*), as well as against a strain of *Methicillin-resistant Staphylococcus aureus (MRSA)* isolated from a patient with chronic ischemia and amputated leg.

Determination of antibacterial activity by microdilution method

Determination of the minimum inhibitory concentration (MIC)

Minimum inhibitory activity against bacteria caused by the action of the 30 POMs (set I) was established by microdilution method standardized by the *National Committee for Clinical Laboratory Standards* (2009), and the MIC of the 7 POMs (set II) was established by the serial microdilution

method in liquid form of nutrient environment. Both tests were conducted on the same bacterial strains that are specific to each set. The reading results were achieved by appreciation the limit (dilution), i.e. the well in which the nanocompounds inhibited bacterial development.

Determination of the minimum bactericidal concentration (MBC)

Minimum bactericidal activity was done only for the POMs belonging to the 1st set, and was determined using the microdilution method on the five bacterial species. The reading was done after 24 hours of incubation by observing the bacterial proliferation in culture medium. POMs were considered having bactericidal activities if they have not enabled the bacterial growth in these culture media.

Results and discussions

There were observed better effects of some POMs, with the bacterial strain- and POM's structure-dependent efficiency by measuring the diameter (in mm) of the inhibition zone of bacterial growth.

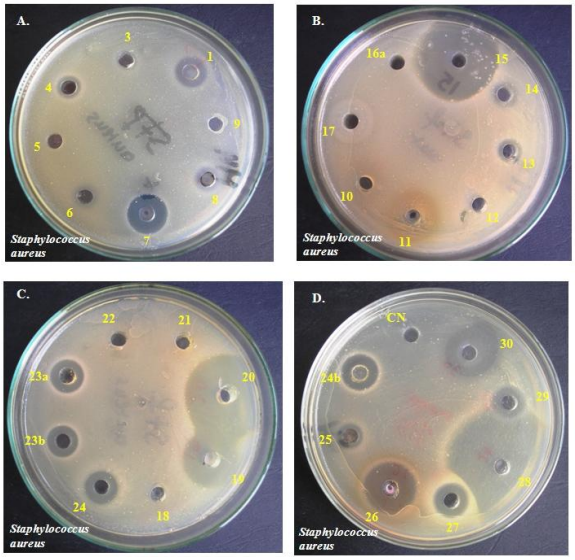

Fig. II.3.2.2. Effect of POMs (1-30) compared to the control (CN, negative control, control group) over the germs of *Staphylococcus aureus* strain (ATCC 6538P); it is observed the presence of zones of inhibition caused by some tested POMs and the absence in others.

The single compound that has proven antibacterial activity against all 5 tested bacterial strains proved to be compound 28 (POM2D = POM-28), maintaining the stronger action than amoxicillin even if sometimes it decreased.

We can mention that only 9 of the 30 tested compounds, at a concentration of 20 µg, did not show antibacterial activity. We assume that the use of higher concentrations of compounds closely related to amoxicillin would improve their antibacterial action.

Conclusions

For testing the antibacterial activity of POMs (set I and set II), taking into consideration pathological aspects, I chose several types of reference Gram-positive (*Staphylococcus aureus, Bacillus cereus*) and of Gram-negative (*Salmonella enteritidis*, *Salmonella typhimurium, Escherichia coli* and *Pseudomonas aeruginosa*) bacterial strains, as well as a strain of *Methicillin-resistant Staphylococcus aureus (MRSA)* isolated from a patient with chronic ischemia and an amputated leg.

1. Characterization of tested POMs were successful in terms of structure-antibacterial activity relationship. Antibacterial effects of these compounds are directly dependent on their structure and bacterial strain tested. Thus, there are compounds that do not inhibit bacterial growth (some POMs with monolacunary Keggin structure), while in the case of trilacunary Keggin and trilacunary/sandwich Keggin structures bacteria did not show resistance. Clusters in general (POM BI-19, 20, 28) and POMs with pseudo-Keggin trilacunary/sandwich structure (POM BI-26) exhibited the most powerful antibacterial effect on all tested bacterial strains even when used in small quantities (20 μg). Its efficiency was higher than that of tested antibiotic (25 μg amoxicillin) and was caused by the $[Sb^{III}W_9O_{33}]^{9-}$ constitutive unit of the pseudo –Keggin structure. Some POMs presented bacteriostatic effect, but not bactericidal.

2. Simple non-complexed butyl-ammonium salts presented a weaker antibacterial effect on all tested bacterial strains compared to those with butyltin fragments. We can argue that the pseudo-Keggin's constitutive unit $[Sb^{III}W_9O_{33}]^{9-}$ is responsible for the very good antibacterial activity exhibited by the pseudo-Keggin trilacunary/sandwich-structured POMs (POM BI-20, 26, 27, 28).

3. In addition, the POM BI-28 cluster complexed with butyl-tin chloride was associated with an intense antibacterial action. In our opinion, this was caused by the $[Sb^{III}W_9O_{33}]^{9-}$ pseudo-Keggin's constitutive unit, as well as by the three butyltin organometallic fragments in the cluster's structure.

4. Five of the seven POMs in the 2nd set demonstrated competitive antibacterial effects compared to nine antibiotics, against both Gram-positive (*S. aureus* and *B. cereus*) and Gram-negative (*E. coli, S. enteritidis, S. typhimurium, P. aeruginosa*) bacterial species, and also (very important) against antibiotic-resistant microbial strains (*MRSA* and *P. aeruginosa*).

5. Antibacterial effects of five of the 2nd set POMs (1-5) were due to their chemical structure: heteropolyoxotungstates with pseudo-Keggin sandwich structures containing Bi^{3+} as heteroatoms and three gaps "filled" with different transitional metals cations. The last two POMs of the 2nd set (6-7)

presented very weak antibacterial activity: POM 6 (containing Fe^{3+}) was effective against *P. aeruginosa* and *B. cereus*, while POM 7 (containing Fe^{2+}) exhibited no antibacterial effects.

3.3. Antitumor activity of synthesized polyoxometalates - in vitro studies

Introduction

The antitumor activity of hepta- or hexa-tungsten/molybdate POMs was found to be stronger than that of certain cytostatics (cisplatin, 5-fluorouracil, gemcitabine), testing being carried out on tumor cell lines isolated from tumors of patients diagnosed with different types of cancer: pulmonary, gastric, pancreatic and breast cancer [107-109, 113, 115]. By inhibiting ATP synthesis, POMs diminish the mitochondrial activity and in the end activate cell apoptosis. Some pharmacokinetic and pharmacodynamic properties of polyoxometalates justify the study of their cytotoxic potential.

This chapter presents the results (summarized in Figure II.3.3.1) achieved by *in vitro* investigations on two cell lines (HUVEC and HeLa), evaluating the antitumor potential of heteropolyoxomolibdates compared to that of heteropolyoxotungstates as well as to that of an Anderson compound.

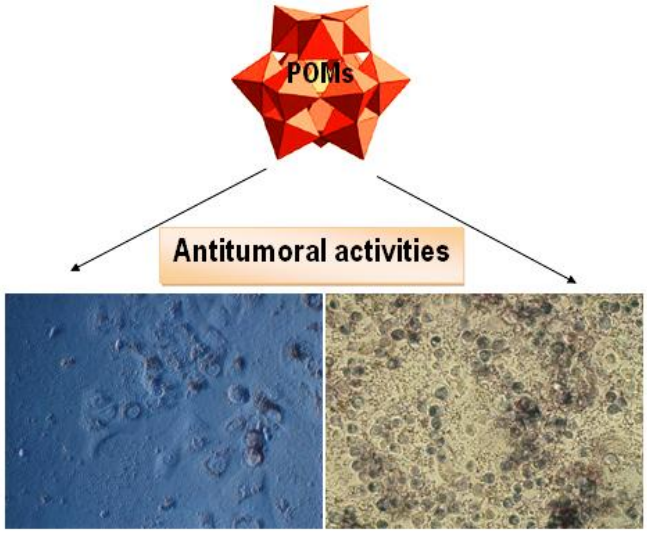

Fig. II.3.3.1. Antitumor effects of polyoxometalates (graphical abstract)

Materials and methods

Biological systems

We used two cell lines, a normal HUVEC endothelial cell line (Human Umbilical Vein Endothelial Cells) and a HeLa cervical cancer tumor line (originating from a HPV 16 infection, i.e. oncogenic Human Papilloma Virus 16 serotype).

Preparation of the POMs solutions

POMs were solubilized in bidistilled water, ethanol or DMSO (dimethyl sulfoxide) to yield stock solutions that were further diluted in the culture medium from the maximum 10 mg/ml concentration to 0.0125 mg/mL for POMs T2, 19, 20, 21, 22 and 23, and from a maximum concentration of 1 mg/mL to 0.00125 mg/mL for POM T15 and 16. The aqueous solutions were then filtered on sterilized Millipore filters of 0.22 μm porosity.

MTT assays were conducted on HUVEC and HeLa cells when found in the exponential phase of cell growth using 96-well plates. A known number of cells (2x104) were seeded into each well containing 200 μL complete medium. After 16 hours of overnight cultivation, the cells were treated with the substances under study. Each determination was performed in triplicate. After 24 hours of treatment, the medium was aspirated and to each well 100 ml of 1 mg/ml MTT (Thyazolyl Blue Tetrazolium Bromide, Sigma-Aldrich) solution were added.

After the incubation was completed, the MTT solution was aspirated from the wells and formazan crystals were dissolved in 150 μL DMSO (dimethyl sulfoxide)/well to give a color reaction. A BioTek Synergy 2 plate reader was used to measure the optical density at 492 nm.

A Zeiss Axiovert D1 microscope in reverse phase was employed to capture 20x, 40x and 1000x optical microscopy images prior to DMSO solubilization in order to observe morphological changes of treatment-exposed cells. Image acquisition was performed by a MRC color camera using Axiovision Rel 8.6 software.

Statistical analysis was conducted on a GraphPad Prism 5 software. The data were processed using one-way ANOVA analysis "Dunnett's Multiple Comparison Test", stating that $p<0.05$.

Results and discussion

Determination of the antitumoral activity of the heteropolyoxomolibdates

POM M2

200mg/mL stock solutions in bidistilled water were prepared for POM M2. Both HUVEC and HeLa cells showed increased sensitivity to high doses up to 0.5 mg/mL, as shown in Figure II.3.3.2. At these concentrations differences compared to control (untreated) samples were statistically significant ($p<0.0001$).

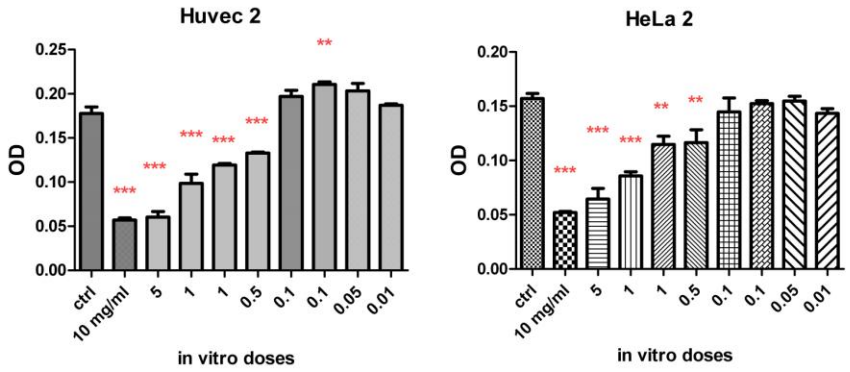

Fig. II.3.3.2. MTT testing of HUVEC and HeLa cells with POM M2 (graphical abstract)

A decrease in the number of tumor cells was observed at high concentrations (10 and 5 mg/mL) via optical microscopy. These cells changed their morphology, becoming bigger and being displayed at the surface of the cultivationplate. Some of them detached from the plate, suggesting the initiation of apoptosis (Figure II.3.3.3 and figure II.3.3.11).

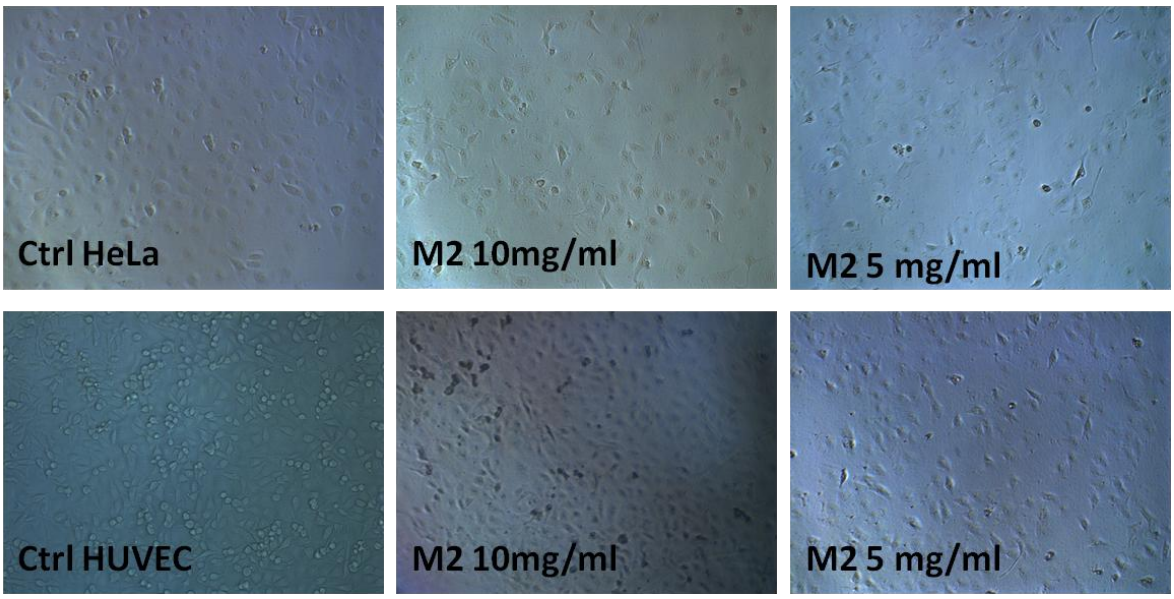

Fig. II.3.3.3. Morphological aspects of HUVEC and HeLa cells treated with POM M2 (10mg/mL and 5 mg/mL).

Optical microscopy revealed that at high concentrations (10 and 5 mg/mL)cells were covered by the resulting precipitate, but at 2,5 mg/mL extremely affected cells in terms of morphology (rounded cells, probably in apoptosis) and number were also visible.

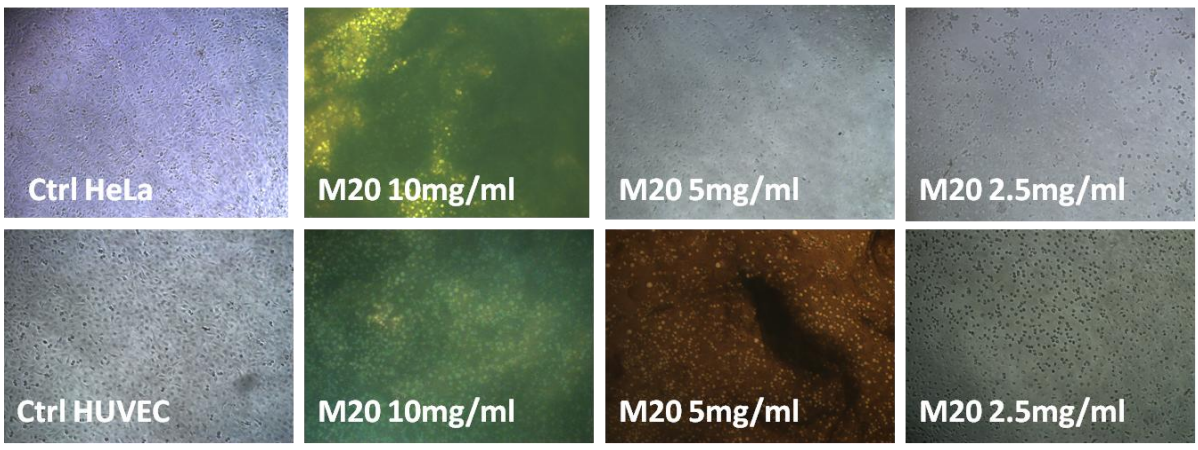

Fig. II.3.3.11. Morphological aspects of HUVEC and HeLa cells treated with POM M20 (10mg/mL and 2.5 mg/mL).

Determination of the antitumor activity of heteropolyoxowtungstates

POM W3

200mg/mL stock solutions in bidistilled water were prepared for POM W3. In the case of the highly hydrosoluble W3, HeLa tumor cells exhibited increased sensitivity compared to normal HUVEC endothelial cells, even at low doses of 1mg/mL (figure II.3.3.22). Differences compared to control (untreated) samples were statistically significant ($p<0.0001$).

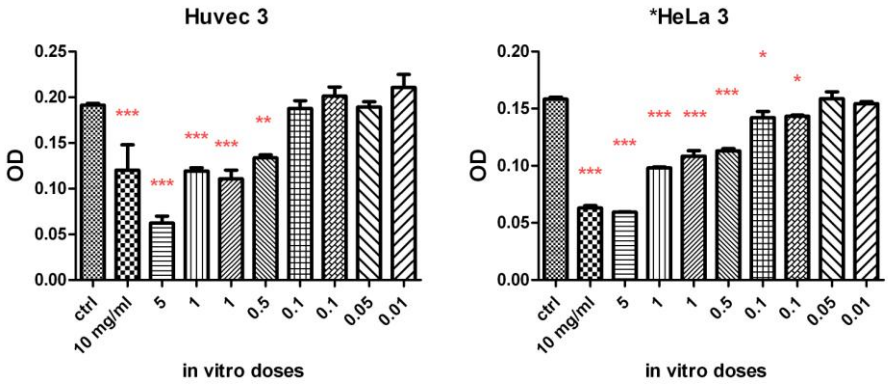

Figure II.3.3.22. MTT testing of HUVEC and HeLa cells treated with POM W3 (graphical abstract)

The same apoptotic cell layout with rounded shapes and decrease in the number of tumor cells were observed at high concentrations (Figure II.3.3.23). Internalisation and accumulation of W3 POM near the perinuclear space is observed, suggesting a nanocompound behavior.

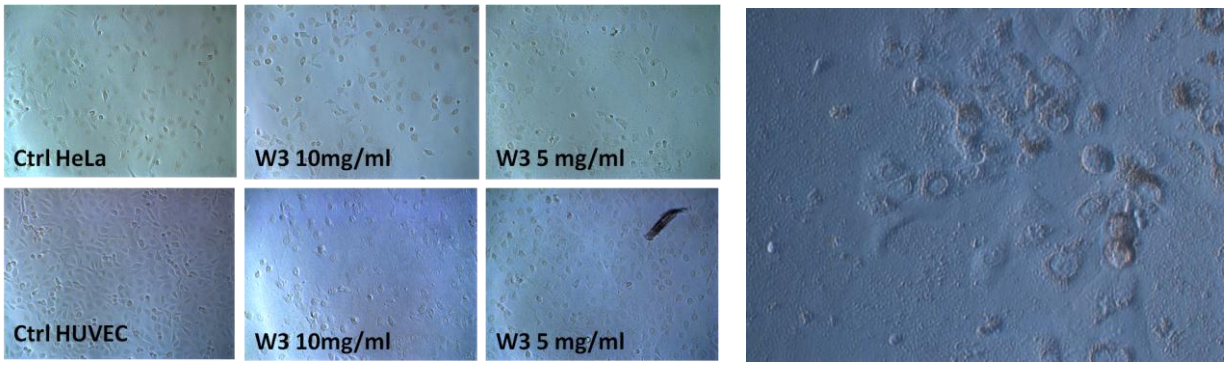

Figure II.3.3.23. Left: Morphological aspect of HUVEC and HeLa cells treated with POM W3 (10mg/mL and 5 mg/mL). Right: Morphological aspect of HUVEC cells treated with POM W3 (40x , images taken after 48 hours).

POM W25

POM W25 is soluble in water and a stock solution of 200 mg/mL was obtained. In the MTT viability assay an intense cytotoxic effect was observed for both cell lines. At low doses POM W25 induced the proliferation of endothelial cells (normal cells, Figure II.3.3.50).

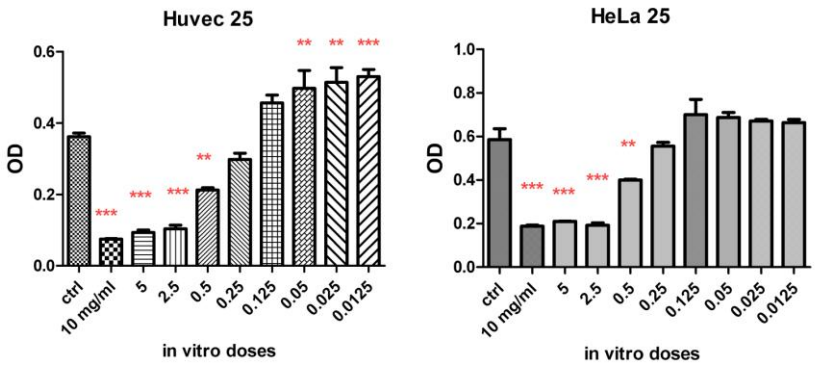

Figure II.3.3.50. MTT test of HUVEC and HeLa cells treated with POM W25 (graphical abstract).

Optical microscopy demonstrated that the cytotoxicity mechanism is determined by inducing intense apoptosis at high doses both tumor cells and endothelial cells (Figure II.3.3.51).

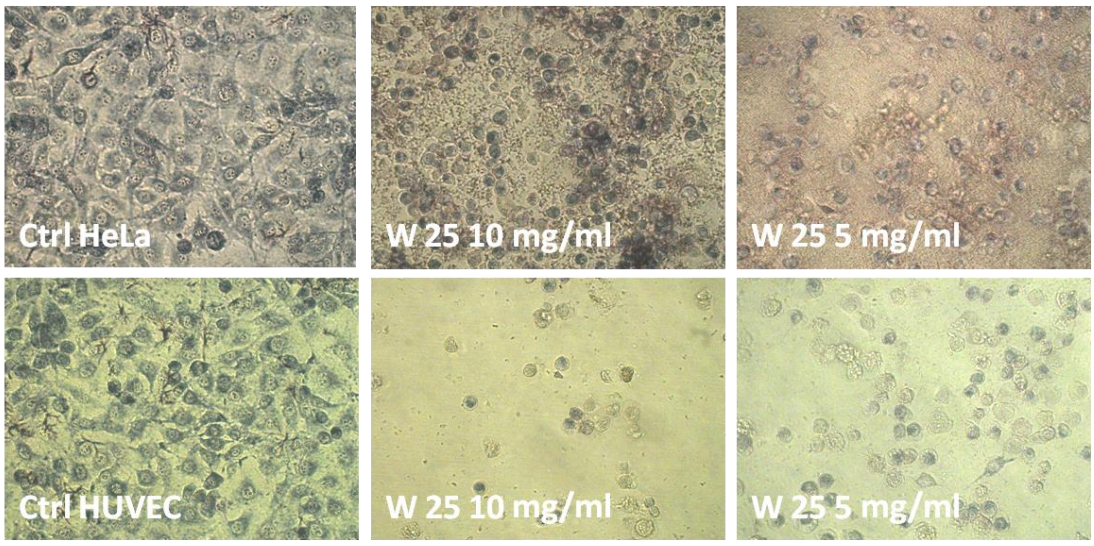

Fig. II.3.3.51. Morphological aspect of HUVEC and HeLa cells treated with POM W25 (10mg/mL and 5 mg/mL).

The typical aspect of apoptosis in HeLa cells following treatment with POM W25 at a dose of 10 mg/mL is observed in Figure II.3.3.52: balooned membrane, chromatin condensation and emergence of nuclear fragments.

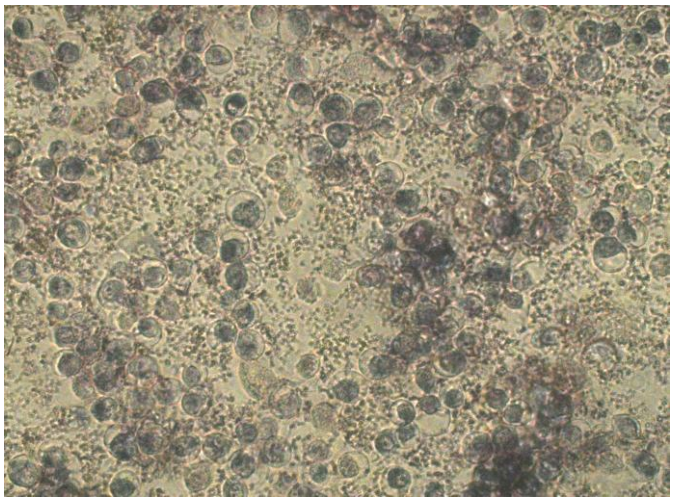

Figure II.3.3.52. Morphological aspect of HeLa tumor cells treated with POM W25 (10mg/mL). Morphological changes typical for apoptosis are observed (400x).

Conclusions

The antitumor activity of heteropolyoxotungstates

The effect of tungsten POMs on both cell lines was different in terms of cell viability and influence upon cell growth/proliferation. Thus, some POMs were found to be essentially non-toxic, not affecting cell proliferation, while other POMs induced the phenomenon of apoptosis, particularly in high doses. The most effective was POM W25, which induced cell death in both tumor and endothelial cells at doses as low as 0.25 mg/mL. At low doses, some of the compounds (POM W10 and W14) led to a small increase in cell proliferation (HeLa tumor cells). These findings are not that bad considering the circumstances, as endothelial cells are the target of anti-tumor treatments as well, the inhibition of tumor neovascularization (an aggravating factor in tumor development and metastasis) being an important goal of anti-tumor treatment.

POM W3 presented a particular feature observed at high magnification optical microscopy. Cells treated for 48 hours with a high POM W3 dose accumulated and concentrated near the perinuclear space of this compound, suggesting a future behavior similar to the nano-type structures. This constitutes a proof regarding the size of these nanocompounds.

The antitumor activity of heteropolyoxomolibdates

All molybdenum POMs exhibited cytotoxic effects on both cell lines, the effect being mainly exerted by initiating the apoptosis phenomenon. This effect was observed at both high and low doses (POM M2, 15, 16). Selectivity based on the cell line was evident. Thus, POM M2, 15, 16, 20 induced a more intense apoptotic effect on HUVEC endothelial cells, while POM M21, 22, 23 acted more strongly on HeLa tumor cells. This opens possible therapeutic selectivity options: direct anti-tumor or anti-angiogenic actions.

A major problem regarded the difficult solubilization of some compounds (POM M19, 20, 21, 22, 23) even in organic solvents and their re-precipitation in the culture medium. Even under such circumstances, the tested POMs exercised their cytotoxic effect, sometimes even at low doses.

GENERAL CONCLUSIONS

1. A number of 50 polyoxometalates including 7 original compounds, 40 synthesized based on literature methodology and 3 commercially-available products were characterized in terms of physico-chemical properties. The newly synthesised 7 polyoxomethalates are:
$(NH_4)_4[NBu_4]_5[Na(BuSn)_3Sb_9W_{21}O_{86}]\cdot 17H_2O$ (POM 2 D=POM BI-28);
$Na_8[La_2(H_2O)_6(Bi_2W_{20}O_{70})]\cdot 37H_2O$ (POM T-8); $Na_{15}[(CeO)_3(OH_2)_2(BiW_9O_{33})_2]\cdot 45H_2O$ (POM T-10); $K_6[SiVW_{11}O_{40}]\cdot 12H_2O$ (POM BI-30); $K_6[Si(VO)Mo_2W_9O_{39}]\cdot 11H_2O$ (POM BI-7);
$Na_5[Fe(H_2O)GeW_{11}O_{39}]\cdot 26H_2O$ (POM BI-24a,b=POM T-26); $Na_{14}[Mn_3(H_2O)_3(SiW_9O_{34})_2]\cdot 25H_2O$ (POM BI-27=POM T-11).

2. The two polyoxometalates with average diameters of 2-4 nm (of which one was newly synthesised) presented a significant hypoglycemic activity, subsequent to the oral treatment in an animal model of STZ - induced diabetes. The tris(vanadyl)-substituted tungsto-antimonate(III)-anion (POM1) tested here proved to be stronger in all respects compared to the tris-butyltin-21-tungsto-9-antimonate(III)-anion (POM2). In addition, one of the main benefits emerging from this study was the dose-dependant low toxicity of these nanocompounds. Based on *in vivo* and *in vitro* studies, we concluded that the two polyoxometalates tested here have exercised their hypoglycemic effects via two different mechanisms concomitently: they prevented the apoptosis of pancreatic β-cells (and the further reduction in the amount of insulin) and stimulated resident stem cell differentiation into new insulin-producing and insulin-secreting pancreatic cells.

3. Characterization of tested POMs were successful in terms of structure-antibacterial activity relationship. Antibacterial effects of these compounds are directly dependent on their structure and bacterial strain tested. Thus, there are compounds that do not inhibit bacterial growth (some POMs with monolacunary Keggin structure), while in the case of trilacunary Keggin and trilacunary/sandwich Keggin structures bacteria did not show resistance. Some POMs exhibited bacteriostatic effects, but were not bactericidal. Simple noncomplexed butyl-ammonium salts presented weaker antibacterial effects on all tested bacterial strains compared to those with butyltin fragments. We can argue that the pseudo-Keggin's constitutive unit $[Sb^{III}W_9O_{33}]^{9-}$ is responsible for the very good antibacterial activity exhibited by the pseudo-Keggin trilacunary/sandwich-structured POMs (POM BI-20, 26, 27, 28). Five of the seven POMs (1-5) in the 2nd set demonstrated competitive antibacterial effects compared to nine antibiotics, against both Gram-positive (*S. aureus* and *B. cereus*) and Gram-negative (*E. coli*, *S. enteritidis*, *S. typhimurium*, *P. aeruginosa*) bacterial species, and also (very important) against antibiotic-resistant microbial strains (*MRSA* and *P. aeruginosa*).

Antibacterial effects of five of the 2nd set POMs (1-5) were due to their chemical structure: heteropolyoxotungstates with pseudo-Keggin sandwich structures containing Bi^{3+} as heteroatoms and three gaps "filled" with different transitional metals cations. The last two POMs of the 2nd set (6-7) presented very weak antibacterial activity: POM 6 (containing Fe^{3+}) was effective against *P. aeruginosa* and *B. cereus*, while POM 7 (containing Fe^{2+}) exhibited no antibacterial effects.

4. A number of 25 POMs from 27 of POMs were characterised in terms of antitumor actvity. The effect of heteropolyoxotungstates on both cell lines (HUVEC and HeLa) was different in terms of cell viability and influence upon cell growth/proliferation. Thus, some POMs were found to be essentially non-toxic, not affecting cell proliferation, while other POMs induced the phenomenon of apoptosis, particularly in high doses. The most effective was POM W25, which induced cell death in both tumor and endothelial cells at doses as low as 0.25 mg/mL. All molybdenum POMs exhibited cytotoxic effects on both cell lines, the effect being mainly exerted by initiating the apoptosis phenomenon. This effect was observed at both high and low doses (POM M2, 15, 16). Selectivity based on the cell line was evident. Thus, POM M2, 15, 16, 20 induced a more intense apoptotic effect on HUVEC endothelial cells, while POM M21, 22, 23 acted more strongly on HeLa tumor cells. This opens possible therapeutic selectivity options: direct anti-tumor or anti-angiogenic actions.

Selective References

1. Berzelius, J.J.; *Poggend. Ann. Phys. Chem.*, **1826**, *6*, 369.

2. Gouzerh, P.; Che, M.; *L'Actualité Chimique*, **2006**, *298*, 1.

3. Keggin, J.F.; *Nature*, **1933**, *131*, 908.

4. Keggin, J.F.; *Nature*, **1933**, *132*, 351.

5. Keggin, J.F.; *Proc. Roy. Soc. A*, **1934**, *144*, 75.

6. Pope, M.T.; *Heteropoly and Isopoly Oxometalates*, Springer, Berlin, Heidelberg, New York, **1983**.

7. Pope, M.T.; Müller, A.; *Angew. Chem. Int. Ed.*, **1991**, *30*, 34.

8. Marcu, Gh.; Rusu, M.; *Chimia polioxometalaţilor*, Ed. Tehnică, București, **1997**.

9. Yamase, T.; *Polyoxometalates: from Platonic Solids to Anti-Retroviral Activity*, Pope, M.T.; Müller, A. (eds), Kluwer Academic Publishers, Dordrecht, Netherlands, **1994**.

10. Lindqvist, I.; *Arkiv Kemi*, **1950**, *2*, 325.

11. Lindqvist, I.; *Arkiv. Kemi*, **1950**, *2*, 349.

12. Anderson, J.S.; *Nature*, **1937**,*140*, 850.

13. Evans Jr., H.T.; *J. Am. Chem. Soc.*, **1948**, *70*, 1291.

14. Wells, A.F.; *Structural Inorganic Chemistry*, Ist Ed, Clarendon Press, Oxford, **1945**, 344.

15. Dawson, B.; *Acta Cryst.*, **1953**, *6*, 113.

16. Clayette, P.; Dormont, D.; *Polyoxometalates: from Platonic Solids to Anti-Retroviral Activity*, Pope, M.T.; Müller, A. (eds), Kluwer Academic Publishers, Dordrecht, Netherlands, **1994**, 387.

17. *Polyoxometalate Chemistry from Topology via Self-Assembly to Applications*, Pope, M.T.; Müller, A. (eds), Kluwer Academic Publishers, Dordrecht, Netherlands, **2001**.

18. *Polyoxometalate Chemistry for Nano-Composite Design*, Yamase, T.; Pope, M.T. (ed), Kluwer Academic/Plenum Publishers, New York, **2002**.

19. *Polyoxometalate Molecular Science*, Borras-Almenar, J.J.; Coronado, E.; Müller, A.; Pope, M.T. (eds), *NATO Science Series II*, Vol. 98, Kluwer Academic Publishers, Dordrecht, Netherlands, **2003**.

20. Fan, D.; Hao, J. Polyoxometalate-Based Assembly. In *Self-Assembled Structures. Properties and Applications in Solution and on Surfaces.* Hao, J. (ed), CRC Press Taylor&Francis Group, Boca Raton, 2011, 141–174.

21. Müller, A.; Peters, F.; Polyoxometalates: Very Large Clusters – Nanoscale Magnets. *Chem. Rev.* **1998**, *98*, 239.

22. Long, D.L.; Burkholder, E.; Cronin, L. *Chem. Soc. Rev.*, **2007**, *36*, 105.

23. Long, D.L.; Tsunashima, R.; Cronin, L.; *Angew. Chem. Int. Ed.*, **2010**, *49*, 1736.

24. Müller, A.; Peters, F.; Pope, M.T.; Gateschi, D.; *Chem. Rev.*, **1998**, *98*, 239.

25. Müller, A.; Kogerler, P.; Bulletin of the Polish Academy of Sciences, Chemistry, **1998**, 46, 207.

26. Müller, A.; Fenske, D.; Kogerler, P.; *Curr. Op. Solid State Mat. Sci*., **1999**, *4*, 141.

27. Choi, H.; Kwon, Y.; Han, O.; *Chem. Mater*., **1999**, *11*, 1641.

28. Caruso, F.; Kurth, G.D.; Dirk, G.; Volkmer, D.; Koop, M.J.; Muller, A.; *Langmuir*, **1998**, *14*, 3462.

29. Polarz, S.; Smarsly, B.; Goltner, C.; Antonietti, M.; *Adv. Maters*, **2000**, *12*, 1503.

30. Muller, A.; Kogerler, P.; Bogge, H.; *Structure and Bonding*, **2000**, *96*, 203.

31. Ribot, F.; Sanchez, C.; *Inorg. Chem*., **1999**, *20*, 327.

32. Kurth, G. D.; Lehmann, P.; Volkmer, D.; Muller, A.; Schwahn, D.; *J. Chem. Soc*., *Dalton Trans.*, **2000**, *21*, 3989.

33. Yang, W.; Xiang, L.; Lu, X.; Hong, C.; Zhuang, H.; Huang, J.; *Inorg. Chem.*, **2000**, *39*, 2706.

34. Cronin, L.; Beugholt, C.; Muller, A.; *Theochem.*, **2000**, *500*, 181.

35. Tang, Z.; Shaoqin, L.; Wang, E.; Dong, S.; *Langmuir*, **2000**, *16*, 4946.

36. Wang, X.; Liu, L.; Zhang, G.; Jacobson, A.; *Chem. Commun.*, **2001**, *23*, 2472.

37. Kurth, D.G.; Lehmann, P.; Volkmer, D.; Colfen, H.; Koop, M.J.; Muller, A.; Du Chesne, A.; *Chem. Eur. J.*, **2000**, *6*, 385.

38. Sanchez, C.; De Soler-Illia, G.J.; Ribot, F.; Lalot, T.; Mayer, C.R.; Cabuil, V.; *Chem. Mat.*, **2001**, *13*, 3061.

39. Xu, L.; Mingqiang, L.; Wang, E.; *Mat. Lett.*, **2002**, *54*, 303.

40. Polarz, S.; Smarsly, B.; Antonietti, M.; *Chem. Phys. Chem*, **2001**, *2*, 457.

41. Wang, Y.; Wang, X.; Changwen, H.; *J. Coll. Interf. Sci*., **2002**, *249*, 307.

42. Liu, S.; Kurth, D.; Volkmer, D.; *Chem. Commun.*, **2002**, *9*, 976.

43. Mayer, C.R.; Neveu, S.; Cabuil, V.; *Angew. Chem*., **2002**, *41*, 501.

44. Yamase, T.; Prokop, P.; *Angew. Chem.*, **2002**, *41*, 466.

45. Rusu, D.; Bâlici, S.; *Polioxometalaţii. Aplicaţii biomedicale*, Ed. Casa Cărţii de Ştiinţă, Cluj-Napoca, România, **2013**.

46. Zou, N.; Chen, W.L.; Li, Y.G.; Liu, W.L.; Wang, E.B.; *Inorg. Chem. Commun.*, **2008**, *11*, 1367.

47. Wu, H.; *J. Biol. Chem.*, **1920**, *43*, 189.

48. Tézé, A.; Hervé, G.; *J. Inorg. Nucl. Chem.*, **1977**, *39*, 999.

49. Rusu, D.; Crăciun, C.; *Cercetări fizico-chimice în domeniul polioxometalaților complecși*, Ed. Casa Cărții de Știință, Cluj-Napoca, **2006**.

50. Klemperer, W.G.; Shum, W.; *J. Am. Chem. Soc.*, **1978**, *100*, 4891.

51. Jahr, K.F.; Fuchs, J.; *Chem. Ber.*, **1963**, *96*, 2457.

52. Rusu, M.; Marcu, Gh.; Rusu, D.; Roșu, C.; Tomșa, A.R.; *J. Radioanal. Nucl. Chem.*, **1999**, *242*, 467.

53. Santoni, M.P.; Pal, A.K.; Hanan, G.S.; Tang, M.C.; Furtosa, A.; Hasenknopf, B.; *Dalton Trans.*, **2014**, *43*, 6990.

54. Pătruț, A.; Bőgge, H.; Forizs, E.; Rusu, D.; Lowy, D.A.; Mărgineanu, D.; Naumescu, A.; *Rev. Roum. Chim.*, **2010**, *55*, 865.

55. Khoshnavazi, R.; Nicolò, F.; Rudbari, H.A.; Naseri, E.; Aminipour, A.; *J. Coord. Chem.*, **2013**, *66*, 1374.

56. Semenovskaya, E.N.; *Zh. Anal. Khim.*, **1986**, *41*, 1925.

57. Parker, G.A.; *Analytical Chemistry of Molybdenum*, Springer-Verlag, New-York, **1983**.

58. Semenovskaya, E.N; *J. Anal. Chem. USSR (Engl. Transl.)*, **1986**, *41*, 1339.

59. Hill, C.L.; Prosser-McCartha, C.M.; *Coord. Chem. Rev.*, **1995**, *143*, 407.

60. Zhai, F.; Li, D.; Zhang, C.; Wang, X.; Li, R.; *Europ. J. Med. Chem.*, **2008,** *43*, 1911.

61. Yamase, T.; Fujita, H.; Fukushima, K.; *Inorg. Chim. Acta*, **1988**, *151*, 15.

62. Yamase, T.; *Polymeric Materials Encyclopedia: Synthesis, Properties and Applications*, J.C. Salamone Eds., CRC Press Inc., Boca Raton, Florida, **1996**, 365.

63. Cindric, M.; Veksli, Z.; Kamenar, B.; *Croat. Chem. Acta*, **2009**, *82*, 345.

64. Rhule, J.T.; Hill, C.L.; Judd, D.A.; Schinazi, R.F.; *Chem. Rev.*, **1998**, *98*, 327.

65. Hasenknopf, B.; *Front. Biosci.*, **2005**, *10*, 275.

66. Cibert, C.; Jasmin, C.; *Biochem. Biophys. Res. Commun.*, **1982**, *108*, 1424.

67. Berry, J.P.; Galle, P.; *Exp. Mol. Path.*, **1990**, *53*, 255.

68. Cholewa, M.; Legge, G.J.F.; Weigold, H.; Holan, G; Birch, C.; *J. Life Sci.*, **1994**, *54*, 1607.

69. Ni, L.; Greenspan, P.; Gutman, R.; Kelloes, C.; Farmer, M.A.; Boudinot, F.D.; *Antiviral Res.*, **1995**, *32*, 141.

70. Alberts, B.; Johnson, A.; Lewis, J.; Morgan, D., Raff, M.; Roberts, K.; Walter, P.; *Molecular Biology of The Cell*, Garland Science Publising, Inc., Taylor&Francis Group, New York, **2015**.

71. Benga, Gh.; *Introducere în Biologia Celulară şi Moleculară*, Ed. Medicală Universitară „Iuliu Haţieganu", Cluj-Napoca, **2005**.

72. Yamase T.; *J. Mater. Chem.*, **2005**, *15*, 4773.

73. Tajima, Y.; Nagasawa, Z.; Tadano, J.; *Microb. Immun.*, **1993**, *37*, 695.

74. Tajima Y.; *Biomed. Res.*, **2002**, *23*, 115.

75. Tajima, Y.; Nagasawa, Z.; Tanabe, I.; Kusaba, K.; Tadano, J.; *Microb. Immun.*, **1994**, *38*, 639.

76. Fukuda, N.; Yamase, T.; Tajima, Y.; *Biol. Pharm. Bull.*, **1999**, *22*, 463.

77. Yamase, T.; Fukuda, N.; Tajima, Y.; *Biol. Pharm. Bull.*, **1996**, *19*, 459.

78. Inoue, M.; Suzuki, T.; Fujita, Y.; Oda, M.; Matsumoto, N.; Iijima, J.; Yamase, T.; *Biomed. Pharmacother.*, **2006**, *60*, 220.

79. Tajima, Y.; *Biol. Pharm. Bull.*, **2001**, *24*, 1079.

80. Inoue, M; Segawa, K; Matsunaga, S; Matsumoto, N; Oda, M; Yamase, T; *J. Inorg. Biochem.*, **2005**, *99*, 1023.

81. Bae, E.; Lee, J.W.; Hwang, B.H.; Yeo, J.; Yoon, J.; Cha, H.J.; Choi, W.; *Chemosphere*, **2008**, *72*, 174.

82. Kong, Y.; Pan, L.; Peng, J.; Xue, B.; Lu, J.; Dong, B.; *Mat. Lett.*, **2007**, *61*, 2393.

83. Colby, D.W.; Prusiner, S.B.; *Cold Spring. Harb. Perspect. Biol.*, **2011**, *3*, 1.

84. Wille, H.; Shanmugam, M.; Murugescu, M.; Ollesch, J.; Stubbs, G.; Long, J.R.; Safar, J.G.; Prusiner, S.B.; *Proc. Natl. Acad. Sci. USA*, **2009**, *106*, 3740.

85. Raynaud, M.; Chermann, J.C.; Plata, F.; Jasmin, C.; Mathe, G.; *C.R. Acad. Sci., Ser.D*, **1971**, *272*, 347.

86. Bonissol, C.; Kona, P.; Chermann, J.C.; Jasmin, C.; Raynaud, M.; *C.R. Acad. Sci., Ser.D*, **1972**, *274*, 3030.

87. Tsiang, H.; Atanasiu, P.; Chermann, J.C.; Jasmin, C.; *J. Gen. Virol.*, **1978**, *40*, 665.

88. Bussereau, F.; Ermine, A.; *Ann. Virol. (Inst. Pasteur)*, **1983**, *134E*, 487.

89. Souyri-Corporale, M.; Tovey, M.G.; Ono, K.; Jasmin, C.; Chermann, J.C.; *J. Gen. Virol.*, **1984**, *65*, 831.

90. Chermann, J.C.; Sinoussi, F.; Jasmin, C.; *Biochem. Biophys. Res. Commun.*, **1975**, *65*, 1229.

91. Bussereau, F.; Chermann, J.C.; DeClercq, E.; Hannoun, C.; *Ann. Virol.*, **1983**, *134E*, 127.

92. Rozenbaum, W.; Dormont, D.; Spoirre, B.; Vilmer, E.; Gentilini, M.; Griscelli, C.; Montagnier, L.; Barre-Sinoussi, F.; Chermann, J.C.; *Lancet*, **1985**, *1*, 450.

93. Moskovitz, B.L.; *Antimicrob. Agents Chemother.*, **1988**, *32*, 1300.

94. Take, Z.; Tokutake, Y.; Inoue, Y.; Yoshida, T.; Yamamoto, A.; Yamase, T.; Nakamura, S.; *Antiviral Res*., **1991**, *15*, 113.

95. Inouye, Y.; Tokutake, Y.; Yoshida, T.; Seto, Y.; Hujita, H.; Dan, K.; Yamamoto, A.; Nishiya, S.; Yamase, T.; Nakamura, S.; *Antiviral Res.*, **1993**, *20*, 317.

96. Weeks, M.S.; Hill, C.L.; Shinazi, R.F.; *J. Med. Chem.*, **1992**, *35*, 1216.

97. Blasecki, J.W.; Polyoxometalates: from Platonic Solids to Anti-retroviral Activity, Kluwer Acad.Pub., Dordrecht, **1994**, 373.

98. Flutsch, A.; Schroeder, T.; Grutter, M.G.; Patzke, G.R.; *Bioorg. Med. Chem. Lett.*, **2011**, *21*, 1162.

99. Sarafianos, S.G.; Kortz, U.; Pope, M.T.; Modak, M.J.; *Biochem. J.*, **1996**, *319*, 619.

100. Wang, J.; Qu, X.; Qi, Y.; Li, J.; Song, X.; Li, L.; Yin, D.; Xu, K.; Li, J.; *PLoS ONE*, **2014**, *9(6):e98292*.

101. De Clercq, E.; *Biochim. Biophys. Acta*, **2002**, *1587*, 258.

102. Liu, J., Mei, W.J., Xu, A.W., Tan, C.P., Shi, S., Ji, L.N., *Antiviral Res*., **2004**, *62*, 65.

103. Liu, Y.N.; Shi, S.; Mei, W.J.; Tan, C.P.; Chen, L.M.; Liu, J.; Zheng, W.J.; Ji, L.N.; *Eur. J. Med. Chem.*, **2008**, *43*, 1963.

104. Qi, Y.F.; Zhang, H.; Wang, J.; Jiang, Y.; Li, J.; Yuan, Y.; Zhang, S.; Xu, K.; Li, Y.; Li, J.; Niu, J.; Wang, E.; *Antiviral Res.*, **2012**, *93*, 118.

105. Zhang; H., Qi, Y.F.; Ding, Y.; Wang, J.; Li, Q.; Zhang, J.; Jiang, Y.; Chi, X.; Li, J.; Niu, J.; *Bioorg. Med. Chem. Lett.*, **2012**, *22*, 1664.

106. Mukherjee, H.N.; *J. Indian Med. Assoc.*, **1965**, *44*, 477.

107. Yanagie, H.; Ogata, A.; Mitsui, S.; Hisa, T.; Yamase, T.; Eriguchi, M.; *Biomed. Pharmacother.*, **2006**, *60*, 349.

108. Ogata, A.; Mitsui, S.; Yanagie, H.; Kasano, H.; Hisa, T.; Yamase, T.; Eriguchi, M.; *Biomed. Pharmacother.*, **2005**, *59*, 240.

109. Ogata, A.; Yanagie, H.; Ishikawa, E.; Mitsui, S.; Yamashita, A.; Hasumi, K.; Takamoto, S.; Yamase, T.; Eriguchi, M.*; Br. J. Cancer***, 2008,** *98,* 2, 399.

110. ***; *Oxford Handbook of Oncology – Principles of chemotherapy*, Oxford University Press Inc., New York, **2006.**

111. Cruce, M.; Stănoiu, B.; Cruce, R.; Ardelean, A.; Pirici, D.; Pisoschi, C.; *Căi şi Reţele de Semnalizare celulară*, Ed. AIUS, Craiova, **2004**.

112. Moldoveanu, E.; Popescu, L.M.; *Apoptoza – Mecanisme moleculare*, Ed. Universitară „Carol Davila", Bucureşti, **1999**.

113. Prudent, R.; Moucadel, V.; Laudet, B.; Barette, C.; Lafanechere, L.; Hasenknopf, B.; Li, J.; Bareyt, S.; Lacote, E.; Thorimbert, S.; Malacria, M.; Gouzerh, P.; Cochet, C.; *Chem. Biol.*, **2008**, *15*, 683.

114. Niefind, K.; Issinger, O.G.; *Biochim. Biophys. Acta*, **2010**, *1804*, 484.

115. Prudent, R.; Sautel, C.F.; Cochet, C.; *Biochim. Biophys. Acta*, **2010**, *1804*, 493.

116. Sha, J.Q., Li, X., Zhou, Y.H., Yan, P.F., Li, G.M., Wang, C., *Solid State Sci.*, **2011**, *13*, 1972.

117. Tan, R., Pang, X., Wang, H., Cui, S., Jiang, Y., Wang, C., Wang, X., Song, W., *Inorg. Chem. Commun*., **2012**, *25*, 70.

118. Menon, D., Thomas, R.T., Narayanan, S., Maya, S., Jayakumar, R., Hussain, F., Lakshmanan, V.K., Nair, S.V., *Carbohydrate Polymers*, **2011**, *84*, 887.

119. Feng, C., Gan, Q., Liu, X., He, H., *J. Rare Earths*, **2012**, *30*, 467.

120. Liu, X., Gan, Q., Feng, C., *J. Rare Earths*, **2012**, *30*, 604.

121. Yamase, T.; *Mol. Eng.*, **1993**, *3*, 241.

122. Ruzzene, M.; Pinna, L.A.; *Biochim. Biophys. Acta*, **2010**, *1804*, 499.

123. Zhang, H.M.; Wang, Y.Q.; Zhou, Q.H.; Wang, G.L.; *J. Molec. Struc.*, **2009**, *921*, 156.

124. Mioc, U.B.; Todorovic, M.R.; Davidovic, M.; Colomban, Ph.; Holclajtner-Antunovic, I.; *Solid State Ionics*, **2005**, *176*, 3005.

125. Mioc, U.B.; Kuntic, V.S.; Nedic, Z.P.; Filipovic, I.M.; Jelic, S.B.; *J. Serb. Chem. Soc.*, **1996**, *61*, 767.

126. World Health Organization, Diabetes Programme, http://www.who.int/diabetes/en.

127. The Expert Committee on the Diagnosis and Classification of Diabetes Mellitus. Follow-up Report on the Diagnosis of Diabetes Mellitus. *Diabetes Care*, **2003**, *26*, 3160.

128. Richardson, S.J.; Morgan, N.G.; Foulis, A.K.; *Endocr. Pathol.*, **2014**, *25*, 80.

129. Yoon, J. W.; Hee-Sook Jun, H. S.; *Am. J. Therapeut.*, **2005**, *12*, 580.

130. Roglic, G.; Unwin, N.; Bennett, P. H.; Mathers, C.; Tuomilehto, J.; Nag, S.; Connolly, V.; King, H.; *Diabetes Care*, **2005**, *28*, 2130.

131. Ledford, H.; *Nature*, **2013**, *504*, 198.

132. Lenzen, S.; *Diabetologia*, **2008**, *51*, 216.

133. Wankeu-Nya, M.; Florea, A.; Bâlici, S.; Watcho, P.; Matei, H.; Kamanyi, A.; *BMC Complement. Altern. Med.*, **2013**, *13:71*.

134. Vardatsikos, G.; Pandey, N.R.; Srivastava, A.K., *J. Inorg. Biochem.*, **2013**, *120*, 8.

135. Kawabe, K.; Sasagawa, T.; Yoshikawa, Y.; Ichimura, A.; Kumekawa, K.; Yanagihara, N.; Takino, T.; Sakurai, H.; Kojima, Y.; *J. Biol. Inorg. Chem.*, **2003**, *8*, 893.

136. Willsky, G.R.; Chi, L.H.; Godzala III, M.; Kostyniak, P.J.; Smee, J.J.; Trujillo, A.M.; Alfano, J.A.; Ding, W.; Hu, Z.; Crans, D.C.; *Coord. Chem. Rev.*, **2011**, *255*, 2258.

137. Crans, D.C.; Smee, J.J.; Gaidamauskas, E.; Yang, L.; *Chem. Rev.*, **2004**, *104*, 849.

138. Goc, A.; *Cent. Eur. J. Biol. (CEJB)*, **2006**, *1*, 314.

139. Munoz, M.C.; Barbera, A.; Dominguez, J.; Fernandez-Alvarez, J.; Gomis, R.; Guinovart, J.J.; *Diabetes*, **2001**, *50*, 131.

140. Fernandez-Alvarez, J.; Barbera, A.; Nadal, B.; Barcelo-Batllori, S.; Piquer, S.; Claret, M.; Guinovart, J.J.; Gomis, R. *Diabetologia*, **2004**, *47*, 470.

141. Altirriba, J.; Barbera, A.; Del Zotto, H.; Nadal, B.; Piquer, S.; Sanchez-Pla, A.; Gagliardino, J.J.; Gomis, R.; *BMC Genomics*, **2009**, *10:406*.

142. Lyonnet, B.; Martz, M.; Martin, E.; *La Presse Médicale*, **1899**, *32*, 191.

143. Srivastava, A.K.; *Mol. Cell. Biochem.*, **2000**, *206*, 177.

144. Domingo, J.L.; *Biol. Trace Elem. Res.*, **2002**, *88*, 97.

145. Badmaev, V.; Prakash, S.; Majeed, M.; *J. Altern. Complement. Med.*, **1999**, *5*, 273.

146. Thompson, K. H.; Orvig, C.; *J. Inorg. Biochem.*, **2006**, *100*, 1925.

147. Goldfine, A.B.; Patti, M.E.; Zuberi, L.; Goldstein, B.J.; LeBlanc, R.; Landaker, E.J.; Jiang, Z.Y.; Willsky, G.R.; Kahn, C.R.; *Metabolism*, **2000**, *49*, 400.

148. Soveid, M.; Dehghani, G.A.; Omrani, G.R.; *Arch. Iran Med.*, **2013**, *16*, 408.

149. Shechter, Y.; Karlish, S.J.D.; *Nature*, **1980,** *284*, 556.

150. Meyerovitch, J.; Farfel, Z.; Sack, J.; Shechter, Y.; *J. Biol. Chem.*, **1987**, *262*, 6658.

151. Heyliger, C.E.; Tahiliani, A.G.; McNeill, J.H.; *Science*, **1985,** *227*, 1474.

152. Cam, M.C.; Brownsey, R.W.; McNeill, J.H.; *Can. J. Physiol. Pharm.*, **2000**, *78*, 829.

153. Nomiya, K.; Torii, H.; Hasegawa, T.; Nemoto, Y.; Nomura, K.; Hashino, K.; Uchida, M.; Kato, Y.; Shimizu, K.; Oda, M.; *J. Inorg. Biochem.*, **2001**, *86*, 657.